The inhibition of KDM2B promotes the differentiation of basal-like breast cancer cells via the posttranslational destabilization of SLUG

Elia Aguado Fraile[2,4], Evangelia Chavdoula[1], Georgios I. Laliotis[1], Vollter Anastas[1,2,3], Oksana Serebrennikova[2,5], Maria D. Paraskevopoulou[2], and Philip N. Tsichlis[1,2]

[1]Department of Cancer Biology and Genetics, The Ohio State University College of Medicine and the Arthur G. James Comprehensive Cancer Center, Columbus, OH. [2]Tufts University School of Medicine, Boston MA [3]Tufts Graduate School of Biomedical Sciences Program in Genetics, Boston MA.

Running Title. KDM2B regulates the stability of SLUG

Present Address. [4] Agios Pharmaceuticals, Cambridge MA 02139

[5] IT Bio, LLC, Boston MA, 02116

Correspondence. Philip N. Tsichlis. The Ohio State University Wexner Medical Center, 982 Biomedical Research Tower, 460, W. 12th Ave. Columbus OH. 43210. Email: philip.tsichlis@osumc.edu

ABSTRACT

KDM2B is a JmjC domain H3K36me2/H3K36me1 demethylase, which immortalizes cells in culture and contributes to the biology of both embryonic and adult stem and progenitor cells. It also functions as an oncogene that contributes to the self-renewal of breast cancer stem cells by regulating polycomb complexes. Here we show that the silencing of KDM2B results in the downregulation of SNAI2 (SLUG), SNAI1 (SNAIL) and SOX9, which also contribute to the biology of mammary stem and progenitor cells. The downregulation of these molecules is posttranscriptional and in the case of the SNAI2-encoded SLUG, it is due to calpain-dependent proteolytic degradation. Mechanistically, the latter depends on the activation of calpastatin-sensitive classical calpain(s) and on the phosphorylation-dependent inhibition of GSK3 via paracrine mechanisms. GSK3 inhibition sensitizes its target SLUG to classical calpains, which are activated by Ca2+ influx and calpastatin downregulation. The degradation of SLUG, induced by the KDM2B knockdown, promotes the differentiation of breast cancer stem cells in culture and reveals an unexpected mechanism of stem cell regulation by a histone demethylase.

INTRODUCTION

Basal-like breast cancer comprises 15-20% of all breast cancers and is more prevalent in younger women (age <40 years) (Kalimutho et al., 2015). These tumors are defined by the lack of expression of estrogen and progesterone receptors and by the absence of amplification of the epidermal growth factor receptor 2 (Prat et al., 2011). Although basal-like breast cancer is heterogeneous (Prat et al., 2013), the majority of breast cancers of this subtype are characterized by an aggressive clinical course, early relapse after treatment and poor overall survival (Denkert et al., 2017; Kalimutho et al., 2015). The poor prognosis of these tumors is partially due to the lack of effective targeted therapies, which leaves aggressive cytotoxic chemotherapy as the mainstay of treatment (Denkert et al., 2017). The goal of the work presented in this report is to improve our understanding of the biology of this disease, which may lead to the development of novel and more effective therapeutic strategies. Its focus is on KDM2B, an enzyme which tends to be expressed at high levels in basal-like breast cancer, and whose expression correlates with the rate of relapse after treatment (Kottakis et al., 2014).

KDM2B (also known as *NDY1, FBXL10, JHDM1B* or *Fbl10*), encodes a jumonji C (JmjC) domain-containing histone lysine demethylase, which targets histone H3K36me2/me1 and perhaps histone H3K4me3 (Kampranis and Tsichlis, 2009; Pfau et al., 2008; Tsukada et al., 2006; Tzatsos et al., 2009) and histone H3K79 me3/me2 (Kang et al., 2018). In addition to the JmjC domain, which is responsible for its demethylase activity (Pfau et al., 2008), KDM2B contains CXXC and PHD zinc finger domains, an F-box and a leucine-rich repeat (Kampranis and Tsichlis, 2009; Pfau et al., 2008). Functionally, it integrates multiple epigenetic signals by coupling H3K36me2/me1 demethylation with H3K27 trimethylation and H2AK119 ubiquitination (Barrero and Izpisua Belmonte, 2013; Kottakis et al., 2011; Lagarou et al., 2008; Tzatsos et al., 2009). These activities of KDM2B depend on its demethylase activity. However, more recent studies revealed that a variant of KDM2B lacking the JmjC demethylase domain also inhibits the methylation of a subset of CpG islands associated with bivalent developmental genes that are targeted by both KDM2B and the PRC complexes in ES cells (Boulard et al., 2015; Kelsey, 2015).

KDM2B functions as an oncogene in several types of tumors. Following the original discovery of its oncogenic potential in Moloney murine leukemia virus (MoMuLV)-induced rodent T cell lymphomas, where it was found to be activated by provirus integration (Pfau et al., 2008; Tzatsos et al., 2009), it has been shown to function as an oncogene in human lymphoid (Andricovich et al., 2016) and myeloid malignancies (van den Boom et al., 2016) as well as in bladder cancer (Kottakis et al., 2011) (McNiel and Tsichlis, 2017) and pancreatic cancer (Tzatsos et al., 2013), basal-like breast cancer (Kottakis et al., 2014), gliomas (Wang et al., 2018) and prostate cancer (Zacharopoulou et al., 2018). The oncogenic potential of KDM2B is mediated by multiple mechanisms. Our early studies revealed that, when overexpressed in normal mouse embryo fibroblasts, KDM2B stimulates cell proliferation and blocks replicative senescence by promoting the phosphorylation of Rb and by blocking the cell cycle inhibitory effects of $p21^{CIP1}$ (Pfau et al., 2008). Subsequently, we and others showed that the ability of KDM2B to stimulate the cell cycle and to block senescence may also be due to the repression of $p16^{INK4A}$ and $p15^{INK4B}$, which it achieves by acting in concert with EZH2 (He et al., 2008; Tzatsos et al., 2009). Our studies addressing the effects of the KDM2B knockdown in a set of ten cancer cell lines, showed that in addition to the inhibition of the cell cycle, which was common to all, the knockdown of KDM2B also induced apoptosis in some (Kottakis et al., 2014).

Our early studies addressing the role of KDM2B in cellular metabolism revealed that KDM2B promotes the expression of a set of antioxidant genes, including aminoadipate-semialdehyde synthase (Aass), NAD(P)H quinone dehydrogenase 1 (Nqo1), peroxiredoxin 4 (Prdx4) and serpin family B member 1b (Serpinb1b), and protects cells from oxidative stress (Polytarchou et al., 2008). More recent studies also showed that KDM2B inhibits the expression of pyruvate dehydrogenase (PDH), shifting cellular metabolism toward aerobic glycolysis and glutaminolysis. The same studies showed that KDM2B upregulates aspartate carbamoyltransferase (ACT), and as a result, it promotes pyrimidine biosynthesis (Yu et al., 2015).

KDM2B plays an important role in the self-renewal and differentiation of both normal and cancer stem cells. First, KDM2B is expressed at high levels in embryonic and adult stem cells. Its overexpression in adult somatic cells promotes their reprogramming to induced pluripotent stem cells (iPSCs) (Liang

et al., 2012; Wang et al., 2011) and its overexpression in fibroblasts contributes to their reprogramming into hepatocyte-like cells (Zakikhan et al., 2016). Other studies provided evidence that KDM2B promotes the self-renewal of hematopoietic and chondrogenic stem cells (Andricovich et al., 2016; Gao et al., 2013; Konuma et al., 2011; Wang et al., 2015) and the commitment of hematopoietic cells toward the lymphoid cell lineage (Andricovich et al., 2016). Our studies focusing on cancer stem cells, revealed that KDM2B is induced by FGF-2, and that it functions in concert with the histone H3K27 methyltransferase EZH2 to repress the expression of a set of microRNAs, which target multiple components of polycomb repressive complex 1 (PRC1) (BMI1 and RING1B) and polycomb repressive complex 2 (PRC2) (EZH2and SUZ12). The repression of these microRNAs results in the upregulation of their polycomb targets. These in turn, promote the self-renewal and inhibit the differentiation of cancer stem cells. Of the microRNA targets of KDM2B and EZH2 particularly interesting is miR-101, an established regulator of EZH2. The repression of miR-101 via the concerted action of KDM2B and EZH2, results in the upregulation of EZH2 and the enhancement of the miR-101 repression. The KDM2B-EZH2/miR-101/EZH2 loop ultimately results in a stable but reversible transition of the cells from a state of high miR-101 and low EZH2 expression, to a state of low miR-101 and high EZH2 expression. Here it is important to note that the repression of the microRNAs that target the listed components of the polycomb complexes depends on the demethylase activity of KDM2B, as evidenced by the fact that overexpression of a catalytically-inactive KDM2B does not promote the recruitment of EZH2 to the miR-101 promoter and the repression of miR-101. However, since both KDM2B and EZH2 are required for the KDM2B microRNA repressive function, EZH2 alone cannot rescue the PRC1 and PRC2 downregulation phenotype elicited by the knockdown of KDM2B (Kottakis et al., 2014; Kottakis et al., 2011).

Given the importance of KDM2B in normal and breast cancer stem cells, we initiated studies to investigate its role in the regulation of SLUG (*SNAI2*), SNAIL (*SNAI1*) and SOX9, which have also been linked to the biology of normal and neoplastic mammary stem cells. Earlier studies had shown that SLUG is expressed in the basal myoepithelial layer of the adult mammary gland and that cells expressing SLUG possess stem cell properties (Guo et al., 2012; Spike et al., 2012). In addition,

transient overexpression of SLUG in luminal progenitor cells, sufficed to reprogram them into mammary stem cells (MaSCs) (Guo et al., 2012). Finally, differentiation of basal/myopithelial cells into luminal cells was associated with the downregulation of SLUG (Guo et al., 2012; Skibinski et al., 2014). Other studies revealed that ectopic expression of SNAIL, a transcription factor closely related to SLUG, also contributes to the reprogramming of luminal cells into basal/myoepithelial cells (Guo et al., 2012).These findings, viewed in the context of the information presented in the preceding paragraphs, suggested a functional relationship between SLUG, SNAIL and KDM2B. The role of SOX9 in the regulation of mammary cell differentiation was suggested by in vivo studies showing that SOX9 is expressed in a subpopulation of cells in the basal/myoepithelial layer of the mammary ducts and that some of these cells express both SLUG and SOX9 (Guo et al., 2012). In addition, SOX9 complemented the ability of SLUG to reprogram fully differentiated luminal cells into cells with stem cell properties (Guo et al., 2012). Thus, whereas SLUG alone fails to reprogram fully differentiated mammary epithelia, the combined expression of SLUG and SOX9 in these cells gives rise to mammary stem cells which assemble to form solid organoids in Matrigel cultures and to produce a complete mammary ductal tree in the murine mammary gland reconstitution assay (Guo et al., 2012).

In this report we examined the effects of the knockdown of KDM2B on the expression of SLUG, SNAIL and SOX9 in human mammary gland-derived cell lines and we showed that all three proteins are downregulated via posttranscriptional mechanisms. Focusing on SLUG, we also showed that the knockdown of KDM2B promotes its degradation by calpains 1 and 2, which are activated by upregulation of intracellular Ca2+ and calpastatin downregulation, both of which are induced by the KDM2B knockdown. Importantly, the sensitivity of SLUG to calpain-mediated degradation was enhanced by phosphorylation-induced GSK3β inactivation, which is also induced by the knockdown of KDM2B. SLUG is partially protected from calpain degradation by GSK3β-dependent phosphorylation and this protection is effectively abolished in cells in which KDM2B is depleted because the depletion of KDM2B promotes the inhibitory phosphorylation of GSK3β. Although the inhibition of GSK3β and the activation of calpain synergize in cells in which KDM2B was knocked down, by converging to degrade SLUG, we also present evidence showing that the inhibition of

GSK3β alone is sufficient to partially destabilize SLUG, and to promote mesenchymal to epithelial transition (MET) and differentiation of mammary epithelial cell lines. The question how a histone demethylase regulates pathways targeting the stability of SLUG was also addressed by co-cultivation experiments which provided solid evidence that these pathways are regulated by paracrine signals induced when KDM2B is knocked down.

RESULTS

KDM2B regulates the expression of SLUG (*SNAI2*), SNAIL (*SNAI1*) and *SOX9* postranscriptionally

To determine whether KDM2B regulates the expression of SLUG, SNAIL and SOX9, we knocked down KDM2B in six immortalized or transformed cell lines derived from the human mammary gland and we examined the effects of the knockdown on the expression of these molecules, both at the RNA and the protein level. This resulted in a dramatic downregulation of SLUG and SNAIL in all the cell lines and of SOX9 in some. Given that the RNA levels of these genes were upregulated rather than downregulated, we conclude that their downregulation was due to posttranscriptional mechanisms (Fig 1A, 1B and S1A).

In parallel experiments, we showed that the overexpression of wild type KDM2B promotes SLUG expression in MDA-MB-231 and MDA-MB-436 cells, but not in MCF-10A cells (Fig 1C). We conclude that KDM2B overexpression indeed upregulates SLUG in tumor cell lines. Its failure to do so in immortalized non-transformed MCF10A cells, is perhaps due to the expression of KDM2B in these cells at levels sufficient to achieve its maximum effect on SLUG expression. Remarkably, overexpression of wild type KDM2B in the luminal breast cancer cell lines T47D and MCF-7 resulted in SLUG downregulation rather than upregulation (Fig S1B), suggesting that the regulation of SLUG by KDM2B described in this report, may be specific for basal-like breast cancer. The specificity was also supported by data on the survival of TCGA patients with breast cancer, who showed that the high expression of KDM2B correlates with poor prognosis only in patients with basal-like triple

negative breast cancer, and that in patients with luminal or HER2-positive breast cancer, it is a favorable prognostic indicator (Fig S1C)

The information on the regulation of SNAIL and SOX9 by KDM2B was presented here to show that KDM2B controls several regulators of mammary stem and progenitor cells, and therefore has a major role in the biology of these cells. In subsequent experiments we focus on SLUG, because SLUG is a critical regulator of mammary stem and progenitor cells, with SNAIL and SOX9 serving accessory roles (Guo et al., 2012).

KDM2B regulates the stability of SLUG.

To determine the mechanism(s) of the posttranscriptional regulation of SLUG by KDM2B we first examined whether KDM2B stabilizes SLUG. To address this question we transduced MDA-MB-231 and MCF10A cells with shKDM2B or shControl constructs. The transduced cells were treated with the protein synthesis inhibitor Cycloheximide (CHX) and the protein levels of SLUG were monitored over time by western blotting. The results revealed that SLUG is less stable in shKDM2B-transduced cells (Fig 2A and S2) and suggested that KDM2B indeed stabilizes SLUG.

SLUG is known to undergo ubiquitination and degradation via the proteasome (Wu et al., 2012; Xu et al., 2009). To determine whether the stabilization of SLUG by KDM2B is due to inhibition of its proteasomal degradation, the shControl and shKDM2B-tranduced MDA-MB-231 and MCF10A cells were treated with the proteasome inhibitor Bortezomib and the levels of SLUG were monitored over time by western blotting. As expected, SLUG levels increased in Bortezomib-treated cells. However, the increase was more pronounced in the shControl than in the shKDM2B cells (Fig 2B). We conclude that SLUG is indeed degraded by the proteasome, but its enhanced degradation in shKDM2B-transduced cells is due to a protein degradation pathway other than the proteasomal pathway.

Earlier studies had shown that the proteasomal degradation of SLUG is triggered by the phosphorylation of the protein by GSK3β at four neighboring phosphorylation sites (Ser92, Ser96, Ser100 and Ser104) (Wu et al., 2012; Xu et al., 2009). To validate our data on the shKDM2B-induced

proteasome-independent degradation of SLUG, we transduced MDA-MB-231 cells with constructs of wild type SLUG, or SLUG mutants in which either all four phosphorylatable serines, or two of them (Ser92 and Ser96), were mutated to alanine (SLUG4A and SLUG2A, respectively). Knockdown of KDM2B in these cells resulted in downregulation of both the wild type and mutant SLUG proteins (Fig 2C). These data support the conclusion that the degradation of SLUG in shKDM2B-transduced cells is not mediated by the proteasome. This conclusion was further supported by the observation that shKDM2B promotes the phosphorylation of GSK3α/β at Ser21/Ser9, in all tested cell lines (Fig 3A). Phosphorylation of GSK3 at these sites inhibits the catalytic activity of the kinase, which is required for the proteasomal degradation of SLUG. If SLUG degradation, in KDM2B depleted cells, were proteasome-mediated, the inactivation of GSK3 would stabilize, rather than destabilize the protein.

To determine which GSK3 isoform undergoes phosphorylation in cells transduced with the shKDM2B construct, we probed cell lysates of shControl and shKDM2B-transduced MDA-MB-231 and MCF-10A cells with antibodies that distinguish phosphorylated GSK3α from phosphorylated GSK3β. The results showed that, although the knockdown of KDM2B enhanced the phosphorylation of both isoforms, the enhancement of GSK3β phosphorylation was more pronounced (Fig S3A).

The shKDM2B-induced GSK3β phosphorylation contributes to the destabilization of SLUG.

To determine whether the inhibition of GSK3β promotes the degradation of SLUG, we treated our cell line panel with the GSK3β inhibitor AR-A-014418. Probing cell lysates harvested 48 hours later with the anti-SLUG antibody revealed that, similar to the knockdown of KDM2B, AR-A-014418 also downregulates SLUG (Fig 3B). Moreover, re-expression of wild type GSK3β rescued partially the SLUG downregulation phenotype in shGSK3β-transduced MDA-MB-231 cells. More important, the expression of the non-phosphorylatable S9A GSK3β mutant rescued the SLUG downregulation phenotype fully in shKDM2B-transduced MDA-MB-231 cells and partially in shKDM2B-transduced MCF-10A cells (Fig 3C). The difference in the magnitude of the effect of GSK3β phosphorylation on SLUG expression in MDA-MB-231 and MCF-10A cells, will be addressed by experiments presented later in this report.

Inhibition of the GSK3β catalytic activity promotes mesenchymal to epithelial transition (MET) and the differentiation of basal like breast cancer cell lines.

SLUG expression promotes epithelial to mesenchymal transition (EMT) in MCF-10A cells (Sarrio et al., 2008). Given that inhibition of GSK3β induces a dramatic downregulation of SLUG, we asked whether chemical inhibitors of GSK3β promote mesenchymal to epithelial transition (MET) of these cells. In addition, we questioned whether treatment of MCF-10A cells with GSK3β inhibitors prevents the induction of EMT in TGFβ-treated MCF-10A. To address the first question, we monitored the expression of SLUG, E-Cadherin and Vimentin in MCF-10A cells treated with AR-A-14418 for 7 days. The results showed that, although the SLUG levels returned to almost normal by day 4, after a precipitous drop by day 2, E-Cadherin levels gradually increased, while Vimentin levels gradually decreased (Fig S3B, Left panel). We conclude that GSK3β inhibition indeed promotes MET. To address the second question, we treated MCF-10A cells with TGFβ for 7 days, in the presence or absence of AR-A-14418. The results showed that AR-A-14418 inhibits the induction of SLUG and Vimentin and promotes the upregulation, rather than the downregulation of E-Cadherin (Fig S3B, middle and right panels). We conclude that by interfering with the induction of SLUG, AR-A-14418 inhibits the induction of EMT by TGFβ.

Our earlier studies had shown that KDM2B promotes the self-renewal of cancer stem cells in basal-like breast cancer cell lines and that the knockdown of KDM2B promotes the loss of cancer stem cells and the differentiation of these cell lines toward a luminal phenotype (Kottakis et al., 2014). Given that AR-A-14418 also downregulates SLUG, we questioned whether GSK3β inhibition phenocopies the knockdown of KDM2B. To address this question, we treated MDA-MB-231 cells with AR-A-014418, or DMSO and we monitored the expression of the cancer stem cell markers CD44 and CD24 and the mammary epithelia differentiation markers CD49f and EpCAM, or CD49f and CD24. The cells were treated with 2 μM of AR-A-014418, and they were analyzed by flowcytometry 7 days later. The results showed that AR-A-014418 indeed lowers the abundance of cancer stem cells, as evidenced by the increase in the number of CD44low cells with a positive shift in CD24 expression (Fig S3C, Left panel). In addition, they showed that AR-A-014418 promotes the differentiation from the basal-like to the

luminal phenotype, as evidenced by the increase in the number of CD49flow cells, with a positive shift in the expression of EpCAM or CD24 (Fig S3C, middle and right panels).

The induction of GSK3β phosphorylation in shKDM2B-tranduced cell lines is under the control of complex phosphorylation and dephosphorylation-dependent mechanisms.

The stoichiometry of GSK3β phosphorylation at Ser9 is regulated by kinases that phosphorylate this site and phosphatases that dephosphorylate it. Kinases known to phosphorylate this GSK3β site include Akt, classical PKC family members, SGK, p70S6K and pp90RSK. To determine which of these kinases may be responsible for the basal and shKDM2B-induced phosphorylation of GSK3β, in MDA-MB-231 and MCF10A cells, we treated shControl and shKDM2B-transduced cells with AZD5363 (pan-Akt inhibitor) (Davies et al., 2012), R0-31-8220 (inhibitor of classical PKCs and PKCε) (McKenna and Hanson, 1993), GSK650394 (pan-SGK inhibitor) (Sherk et al., 2008), PF-4708671 (p70S6K inhibitor) (Pearce et al., 2010), or BI-D1870 (pp90RSK inhibitor) (Sapkota et al., 2007). Cell lysates harvested 2 hours later were probed with antibodies that recognize Ser9-phosphorylated or total GSK3β. The results showed that only the inhibitors of Akt and PKC inhibited GSK3β phosphorylation (Fig S4A). However, the inhibition was independent of the KDM2B knockdown. When the same experiment was repeated with parental non-transduced cells harvested at 24 hours from the start of the treatment, we observed that the SGK inhibitor (GSK650394) also interfered with GSK3β phosphorylation (Fig S4B). We conclude that whereas Akt, the classical PKCs and SGK phosphorylate GSK3β in mammary gland-derived cell lines, p70S6K and pp90RSK do not.

A prerequisite for a kinase that has the potential to phosphorylate GSK3β to be responsible for the upregulation of GSK3β phosphorylation in shKDM2B-transduced cells is its upregulation and/or activation, upon the knockdown of KDM2B. Based on this consideration we proceeded to address the role of Akt, classical PKCs and SGK on the induction of GSK3β phosphorylation by shKDM2B. To this end, we monitored the effects of the KDM2B knockdown on the expression and phosphorylation of these kinases. Figure 4A shows that the knockdown of KDM2B increased the phosphorylation of Akt in MDA-MB-231 and MCF-10A cells, but not in the remaining four cell lines, where Akt

phosphorylation was decreased. It is interesting that the changes in the phosphorylation of Akt induced by the knockdown of KDM2B exhibited a perfect negative correlation with changes in the expression of INPP4B, a phosphoinositide phosphatase, which removes the D4 phosphate from the phosphorylated inositol ring of PtIIns3,4-P2 (Gewinner et al., 2009; Li Chew et al., 2015) (Fig 4B). This suggests that the differential regulation of Akt phosphorylation by shKDM2B among different cell lines may be due to the differential effects of shKDM2B on INPP4B expression. To determine the role of PKC isoforms on the induction of GSK3β phosphorylation in shKDM2B-transduced cells, we probed lysates of shControl and shKDM2B cells with a PKC phosphosubstrate antibody (Monteverde et al., 2018). The results in figure 4C revealed inhibition, rather than activation of PKC in all the shKDM2B-transduced cells (Fig 4C). To determine the role of SGK isoforms in the shKDM2B-induced phosphorylation of GSK3β, we probed shCntrl and shKDM2B cell lysates for SGK1, SGK2, SGK3 and phosphoSGK3 (Thr320) and we observed that the knockdown of KDM2B results in the upregulation of SGK2 in MDA-MB-236, HMEC and RMF cells. SGK3 phosphorylation was also induced in MDA-MB-236 cells and HMECs (Fig 4D). We conclude that SGK2 and SGK3 may selectively contribute to GSK3 phosphorylation in some of the tested cell lines. The data in figure 4A-D collectively show that the induction of GSK3β phosphorylation, which is observed in all the shKDM2B-transduced cells, is mediated either by Akt or SGK in different cell lines. The enhanced phosphorylation of SGK3 in MDA-MB-436 cells and HMECs could be explained by the increase in INPP4B in these cell lines, which has been suggested to induce a signaling switch from AKT to SGK activation (Gasser et al., 2014). However, such a switch was not observed in RMFs.

The role of phosphatase inactivation in the enhancement of GSK3β phosphorylation by shKDM2B was addressed in MDA-MB-231 cells in which GSK3β is phosphorylated by Akt, that is activated by shKDM2B. To this end, shControl and shKDM2B-transduced MDA-MB-231 cells were treated with the pan-Akt inhibitor AZD-5363. Monitoring GSK3β phosphorylation for 30 minutes from the start of the treatment, revealed a rapid decline in shControl and a slower decline in shKDM2B-transduced cells (Fig 4E). We conclude that the increase in GSK3β phosphorylation at Ser9 in shKDM2B-

transduced MDA-MB-231 cells is due, at least in part, to the inactivation of phosphatases that dephosphorylate this site.

Two phosphatases, PP1 and PP2A, are known to dephosphorylate GSK3, phosphorylated at Ser9/21 (McCubrey et al., 2014). Both of them are complex multi-subunit metaloenzymes. The PP1 holoenzyme consists of a 38.5 KD catalytic subunit and a regulatory targeting subunit. There are four isoforms of the catalytic subunit (PP1α, PP1β/δ, PP1γ1 and PP1γ2), which are encoded by three different genes (PPP1CA, PPP1CB and PPP1CC respectively). The four isoforms of the catalytic subunit associate with one of approximately 200 regulatory subunits (Peti et al., 2013). The PP2A holoenzyme consists of a 65 KD scaffolding subunit (A), a 36 KD catalytic subunit (C) and a regulatory subunit (B). Whereas the scaffolding A subunit and the catalytic C subunit come in two isoforms each (Aα/Aβ and Cα/Cβ respectively), the regulatory B subunit comes in 26 isoforms, which can be grouped into four subfamilies (B, B', B'' and B'''). Switching between the different isoforms of these subunits determines the subcellular localization and specificity of the phosphatase, and its response to different signals(Kiely and Kiely, 2015) . Using the CPTAC proteomic and phosphoproteomic data for breast cancer (Mertins et al., 2016), we observed a negative correlation between GSK3 phosphorylation at Ser21 and two of the three catalytic subunits of PP1, the two catalytic subunits of PP2A, and several regulatory subunits of both phosphatases (Tables S1 and S2). These observations provide support to the hypothesis that both phosphatases dephosphorylate Ser9/21-phosphorylated GSK3 in breast cancer. More important, some of the catalytic subunits and some of the regulatory subunits of both phosphatases, which either do not correlate, or correlate negatively with GSK3 phosphorylation, switch to a pattern of positive correlation with phosphorylated GSK3 when phosphorylated at specific sites (Tables S1 and S2). We interpret these observations to suggest that subunit phosphorylation at the indicated sites interferes with the ability of these phosphatases to dephosphorylate GSK3-phospho-Ser9/Ser21. The potential involvement of KDM2B in the regulation of PP1 and PP2A subunit phosphorylation and the ability of these phosphorylation events to inactivate the phosphatases will be addressed in future studies.

The knockdown of KDM2B in mammary cell lines destabilizes SLUG via calpain activation.

Data discussed above revealed that the degradation of SLUG in shKDM2B-transduced cells is proteasome-independent. To determine which protease family may be responsible for the destabilization of SLUG in these cells, we treated shControl and shKDM2B-transduced MDA-MB-231 cells with increasing concentrations of three different small molecules, chloroquin (CQ), 3-methyladenine (3-MA), or concanamycin A (ConA), which inhibit autophagy at different stages (Dikic and Elazar, 2018; Mizushima et al., 2010). Monitoring the effects of these treatments on the abundance of SLUG showed that none stabilized SLUG in either shControl or shKDM2B-transduced cells (Fig S5A) Therefore, the downregulation of SLUG following the knockdown of KDM2B was also not due to the activation of autophagy. We next examined the role of calpains by monitoring the cellular levels of SLUG over a 90 minute period in shControl and shKDM2B-transduced MDA-MB-231 and MCF-10A cells treated with a cell-permeable peptide derived from calpastatin (CAST), an endogenous inhibitor of calpain-1, calpain-2 and calpain-9 (Storr et al., 2011a; Storr et al., 2011b; Wendt et al., 2004). The upregulation of SLUG by calpastatin only in shKDM2B-transduced cells (Fig 5A) indicated that calpastatin stabilizes SLUG and suggested that shKDM2B promotes the degradation of SLUG via calpain activation. Using an in vitro assay to measure calpain activity in cell lysates of shControl and shKDM2B-transduced cells confirmed that the knockdown of KDM2B indeed promotes calpain activation (Fig 5B). The activation was reproducibly more robust in MCF10A than in MDA-MB-231 cells (Fig 5B). This observation was consistent with the finding that ectopic expression of the GSK3βS9A mutant rescues the shKDM2B-induced downregulation of SLUG fully in MDA-MB-231 cells and only partially in MCF10A cells (Fig 3C).

To address the mechanism of calpain activation we first examined the expression of calpastatin and the calpastatin-inhibited calpains 1, 2 and 9 by western blotting. The results revealed calpastatin downregulation in all the shKDM2B-transduced cell lines (Fig 5C) and calpain 1 and 2 upregulation in some (HMEC and RMF) (Fig S5B). Calpain 9 was downregulated rather than upregulated in most cell lines, suggesting that it was not contributing to the phenotype. Since activated calpain degrades calpastatin (De Tullio et al., 2000), we also examined the abundance of calpastatin RNA in shControl and shKDM2B cells. The results revealed that calpastatin mRNA was also reduced by shKDM2B (Fig

5D and Fig S5C), which indicates that calpastatin is downregulated at the RNA level, and it is therefore not due to calpain-mediated degradation.

To determine whether the downregulation of calpastatin contributes to the shKDM2B-induced degradation of SLUG, we first knocked down calpastatin in MDA-MB-231 and MCF-10A cells. Western blotting of lysates derived from these and control cells revealed that the knockdown of calpastatin indeed downregulates SLUG in both cell lines (Fig 5E). More important, re-expression of calpastatin in shKDM2B-transduced MDA-MB-231 cells partially restored SLUG expression (Fig 5F).

The partial rescue of SLUG expression by calpastatin suggested that the calpastatin downregulation is one, but not the only factor responsible for the destabilization of SLUG in these cells. Another regulator of calpain activity is Ca^{2+}. To determine whether the knockdown of KDM2B upregulates intracellular Ca^{2+}, we treated shControl and shKDM2B-transduced MDA-MB-231 and MCF10A cells with the calcium indicator Fluo-3. Monitoring the intensity of Fluo-3 staining (59) by flow-cytometry confirmed that shKDM2B indeed upregulates intracellular Ca^{2+} (Fig 5G). To address the role of intracellular Ca^{2+} in calpain activation and the effects of calpain activation by Ca2+ on the abundance of SLUG, we treated MDA-MB-231 and MCF10A cells with increasing concentrations of ionomycin, which upregulates intracellular Ca^{2+} via mechanisms that are independent of the knockdown of KDM2B, and we monitored the effects of these treatments on the activity of calpain (Fig S5D) and on the cellular levels of SLUG (Fig 5H). The results confirmed the activation of calpain by ionomycin and demonstrated that SLUG degradation parallels calpain activation. We conclude that the activation of calpain in shKDM2B-transduced cells is due at least in part to the upregulation of intracellular Ca^{2+}, and that SLUG is a target of calpain.

The proximal mechanism by which the KDM2B knockdown promotes the upregulation of intracellular Ca^{2+} is currently unknown. Given that the gene encoding ORAI1, a store-operated Ca^{2+} channel (Putney et al., 2017) maps immediately upstream of the gene encoding KDM2B, we hypothesized that the knockdown of KDM2B induces a compensatory increase in the expression of both the endogenous KDM2B gene and its immediate neighbor, ORAI1. The cBioportal-analyzed TCGA data

on breast cancer provided support to this hypothesis by showing that the expression of KDM2B and ORAI1 exhibit a strong positive correlation (Spearman correlation coefficient 0.42) (https://www.cbioportal.org). The same data showed that KDM2B and ORAI3 expression exhibit a negative correlation (Spearman correlation coefficient -0.31) (https://www.cbioportal.org), suggesting that KDM2B may also contribute to the steady state Ca^{2+}regulation in breast cancer via ORAI3. The role of KDM2B in the regulation of intracellular Ca^{2+} levels and the consequences of this regulation in breast cancer will be addressed in future studies.

The inhibition of GSK3β and calpain activation synergize to destabilize SLUG

The preceding data raised the question whether GSK3β inhibition in shKDM2B-transduced cells activates calpain. To our surprise, although inhibition of GSK3β downregulates SLUG (Fig 3), it does not downregulate calpastatin and it does not activate calpain (Fig 6A and 6B). Based on these data, we hypothesized that the inhibition of GSK3β and the activation of calpain by shKDM2B, are two parallel processes which converge on SLUG, and that the inhibition of GSK3β may sensitize SLUG to degradation by the activated calpain (Fig S6).

The hypothesis that the phosphorylation of SLUG by GSK3β reduces its sensitivity to calpain cleavage was addressed with the experiment in figure 6C. Wild type SLUG and the nonphosphorylatable mutants SLUG-2A, (S92A/S96/A) and SLUG-4A (S92A/S96AS100/A/S104A) were expressed in, and purified from *E Coli.* The purified proteins were phosphorylated by GSK3β in vitro. Wild type and mutant proteins phosphorylated by GSK3β, or mock-phosphorylated in vitro, were treated with purified calpain 1. Monitoring the calpain-mediated degradation of these proteins by western blotting, revealed that phosphorylation by GSK3β protects wild type SLUG, but not its phosphorylation site mutants (Fig 6C). These results confirmed our original hypothesis by showing that phosphorylation of SLUG by GSK3β partially protects it from degradation by calpain. Therefore, the inhibition of GSK3β via Ser9 phosphorylation renders SLUG more sensitive to calpain-mediated degradation (Fig S6).

The knockdown of KDM2B initiates paracrine mechanisms, which are responsible for both GSK3β phosphorylation and calpain activation.

To address how the knockdown of the histone demethylase KDM2B activates signaling pathways which result in the phosphorylation of GSK3β, the upregulation of intracelular Ca2+ and calpain activation, we probed lysates of shKDM2B and shControl MDA-MB-231, MDA-MB-436 and HMEC cells with an anti-phosphotyrosine antibody (Millipore # 05-321). The results showed that shKDM2B induces significant shifts in tyrosine phosphorylation (Fig 7A), suggesting that shKDM2B may activate these pathways via paracrine mechanisms. The tyrosine kinases that may be activated by the apparent paracrine mechanism have not been positively identified to-date. However, analysis of the reverse phase proteomic array (RPPA) data of the 1014 cases of breast cancer, in the 2019 Firehose TCGA database, revealed significantly higher levels of ErbB2, ErbB2_pY1248, and ErbB3 in tumors with low levels of KDM2B (Fig S7). These data suggest that the knockdown of KDM2B may result in the upregulation and activation of ErbB2 and ErbB3. The receptor tyrosine kinases and the tyrosine phosphorylation pathways activated by the knockdown of KDM2B, will be addressed in future studies.

To confirm that the knockdown of KDM2B induces the degradation of SLUG by activating paracrine signaling, we co-cultivated Red fluorescent protein (RFP)-expressing MDA-MB-231cells transduced with shControl or shKDM2B constructs, with non-labelled parental MDA-MB-231 cells. Knocking down KDM2B in this cell line activates AKT by phosphorylation at Thr308 and Ser473 (Fig 4A). Following cocultivation, we stained the cells with an anti-phosphoAkt (phosphor-Ser473) antibody and we analyzed them by flowcytometry. This revealed that shKDM2B induces AKT phosphorylation not only in the shKDM2B-positive/ RFP-positive, but also in the shKDM2B-negative /RFP-negative cells. (Fig 7B). We conclude that the knockdown of KDM2B activates AKT via paracrine mechanisms, not only in the cells in which KDM2B was knocked down, but also in the neighboring cells.

To determine whether the upregulation of intracellular Ca^{2+} is also induced via paracrine mechanisms, the cells described in the preceding paragraph were treated with Fluo-3 and they were analyzed by flow-cytometry, as described in the supplementary Materials and Methods. Gating the RFP-negative cells, revealed that intracellular Ca^{2+} was again increased not only in cells in which KDM2B was knocked down, but also in their neighbors (Fig 7C). Therefore, both AKT activation and Ca^{2+} influx were induced via paracrine mechanisms (Fig 7D).

DISCUSSION

Our earlier studies had shown that KDM2B, in concert with EZH2, represses the expression of a set of microRNAs which target multiple components of the polycomb complexes PRC1 and PRC2. As a result, KDM2B upregulates the activities of PRC1 and PRC2 and promotes the self-renewal of breast cancer stem cells. As expected from these data, the knockdown of KDM2B depleted breast cancer cell lines of cancer stem cells by promoting their differentiation, in vitro as well as in vivo, in a model of orthotopic transplantation of human breast cancer cell lines into the mammary gland of immunodefficient mice. Given that other studies had shown that the self-renewal and differentiation of mammary epithelial stem cells also depends on SLUG, SNAIL and SOX9 (Guo et al., 2012; Skibinski et al., 2014; Spike et al., 2012), we questioned whether KDM2B also regulates the expression of these molecules. Data presented in this report confirmed this hypothesis and they showed that the regulation of these molecules by KDM2B is postranscriptional. The potential interdependence of the regulation of PRC complexes and SLUG/SNAIL/SOX9 by KDM2B will be addressed in future studies.

Women with mutations in BRCA1 develop triple negative, basal-like mammary adenocarcinomas, a type of tumor that tends to express high levels of KDM2B. Moreover, knockdown of BRCA1 in mammary epithelial cell lines and inactivating oncogenic mutations of BRCA1 promote the upregulation of SLUG by posttranslational mechanisms (Proia et al., 2011).Therefore, the effects of KDM2B expression and BRCA1 mutation on the expression of SLUG in mammary epithelia are similar, raising the question whether KDM2B expression and BRCA1 mutations function in the same pathway. The data presented in this report indicate that the knockdown of KDM2B decreases the levels of SLUG in both BRCA1 wild type cells (MDAMB-231, MCF-10A, HMEC and RMF) and BRCA1 mutant cells (MDAMB-436 and BHMEC). This suggests that if KDM2B and BRCA1 mutations are functionally interdependent, KDM2B would function downstream of BRCA1. Preliminary data from this lab support this interpretation by showing that the knockdown of BRCA1 in MDA-MB-231 cells, a basal-like breast cancer cell line with normal BRCA1, is associated with an increase in the levels of

KDM2B and a decrease in the phosphorylation of GSK3β (Data not shown). The functional relationship between these molecules will be explored in future studies.

The knockdown of KDM2B downregulates SLUG by promoting its degradation (this report). SLUG degradation had been shown earlier to be mediated by the proteasome, downstream of SLUG phosphorylation by GSK3β (Kao et al., 2014; Kim et al., 2012; Wu et al., 2012). We therefore examined the expression and phosphorylation of GSK3β, and to our surprise, we observed that shKDM2B promotes GSK3β inactivation via phosphorylation at Ser9. This observation, combined with the results of additional pharmacologic and genetic studies, confirmed that the shKDM2B-induced SLUG degradation does not depend on the proteasome, but on calpain activation. Further studies showed that calpain activation by shKDM2B was due to the upregulation of intracellular Ca^{2+} and the downregulation of calpastatin. Given that the only calpains inhibited by calpastatin are calpains 1, 2 and 9 (Storr et al., 2011a; Storr et al., 2011b; Wendt et al., 2004), this finding limited the spectrum of calpains that may be activated by shKDM2B and may therefore be responsible for SLUG cleavage. Of these calpains, the expression of calpain 1 and calpain 2 remains unchanged, or increases in shKDM2B-transduced cells, while the expression of calpain 9 decreases in most of the tested cell lines. Based on these findings we conclude that SLUG degradation is mediated primarily by calpains 1 and 2. Overall, our data show that under steady-state conditions, SLUG is degraded via the proteasome. However, when KDM2B is depleted, the slow proteasomal degradation of SLUG is blocked because of GSK3β inhibition and it is replaced by a rapid degradation process that is mediated by calpains 1 and 2.

Our data showing that the knockdown of KDM2B promotes the degradation of SLUG via GSK3β inactivation and calpain1/2 activation raised the question whether the activation of calpains 1 and 2 depends on the inhibition of GSK3β. To our surprise, although inhibition of GSK3β downregulated SLUG, it did not activate calpains 1 and 2. This led us to conclude that GSK3β inhibition and calpain activation are parallel processes, which however may converge on SLUG, and that the inhibition of GSK3β may sensitize SLUG to calpains, by preventing SLUG phosphorylation. The inhibition of calpain-mediated proteolysis by phosphorylation of the target protein had been described previously,

and one of the proteins whose degradation is regulated by this mechanism is GSK3β (Kamei et al., 2007; Lopez-Menendez et al., 2013; Ma et al., 2012; Yuen et al., 2007). Specifically, GSK3β is cleaved by calpain at both its N-terminus and C-terminus and its cleavage is prevented by phosphorylation at Ser-9 and Ser-389 (Ma et al., 2012). Data presented in this report confirmed that calpain-dependent SLUG degradation is indeed inhibited by GSK3β-mediated phosphorylation. The relative contribution of GSK3β inactivation and calpain activation in the degradation of SLUG by shKDM2B may vary between cell lines. This is suggested by the comparison of the magnitude of calpain activation in shKDM2B-transduced MDA-MB-231 and MCF10A cells and the ability of the constitutively-active mutant GSK3β-S9A to rescue the calpain-mediated cleavage of SLUG in the two cell lines. Thus, in MDA-MB-231 cells in which calpain activation was weak (Fig 5B), the rescue by GSK3β-S9A was complete (Fig 3C Left panel), while in MCF10A cells, in which calpain activation was strong (Fig 5B), the rescue was partial (Fig 3C Right panel).

In agreement with earlier observations (Lee and Ro, 2015; Vijay et al., 2019), pharmacological inhibition of GSK3β resulted in SLUG downregulation in basal-like breast cancer cell lines and prevented EMT in cells treated with TGF-β. These observations suggest that inhibition of GSK3β drives mammary cell differentiation, and that it may be a promising strategy for the treatment of basal-like breast cancer. GSK3β inhibitors are currently available and they are being tested in clinical trials for metastatic pancreatic cancer (NCT01632306), other epithelial cancers (NCT01287520) (Gray et al., 2015) and acute leukemia (NCT01214603) (McCubrey et al., 2014).

Treatment of MDA-MB-231 and MCF10A cells with several kinase inhibitors revealed that under steady state conditions, GSK3β is phosphorylated at Ser9, primarily by AKT, PKC and SGK (McCubrey et al., 2014). However, the enhancement of GSK3β phosphorylation at this site in shKDM2B-transduced cells is primarily due to inhibition of its dephosphorylation, with a contribution from AKT, PKC and SGK, which are activated selectively downstream of shKDM2B in different cell lines. AKT for example may contribute to the increase in GSK3β phosphorylation in shKDM2B-transduced MDAMB-231 and MCF-10A cells but not in the other cell lines, probably because of the differential regulation of INPP4B by KDM2B in these cells. Analysis of the breast cancer CPTAC

dataset (Mertins et al., 2016) for correlations between GSK3 phosphorylation at Ser9/21and the abundance of different PP1 and PP2A subunits (total and phosphorylated at various sites), provided evidence suggesting regulatory mechanisms that may be KDM2B-dependent and may contribute to the abundance of GSK3 phosphorylation by targeting PP1 and PP2A (See Tables S1 and S2)

As mentioned in the preceding paragraphs, the loss of GSK3-mediated SLUG phosphorylation renders SLUG sensitive to degradation by calpains 1 and 2, which are also activated when KDM2B is knocked down. Data presented in this report show that calpain activation depends on multiple mechanisms, operating in concert. First, the knockdown induces an increase in the levels of intracellular Ca^{2+}, a signal of calpain activation (Storr et al., 2011a; Storr et al., 2011b). The Ca^{2+}-dependent calpain activation is sustained via the transcriptional downregulation of calpastatin, a natural inhibitor of calpains 1,2 and 9 (Storr et al., 2011a; Storr et al., 2011b; Wendt et al., 2004). Finally, in some tumor cells, the knockdown of KDM2B promoted the upregulation of calpains 1 and 2, which is likely to also contribute to the observed increase in calpain activity. The mechanism by which the knockdown of KDM2B upregulates the intracellular Ca^{2+} levels is currently unknown. However, the correlations we observed, by analyzing the TCGA data on breast cancer, between the abundance of KDM2B and the abundance of ORAI1 and ORAI3 (see results section) suggest the potential contribution of these Ca^{2+} channels on the KDM2B-dependent Ca^{2+} regulation.

Experiments addressing the important question of how the knockdown of a histone demethylase induces GSK3β phosphorylation and calpain activation, revealed that both events depend on shKDM2B-induced paracrine signaling. Specifically, knocking down KDM2B in RFP-expressing MDA-MB-231 cells cocultivated with parental RFP-negative MDA-MB-231 cells, resulted in AKT phosphorylation and Ca2+ influx not only in the RFP-positive cells in which KDM2B was knocked down, but also in the RFP-negative parental cells. The shKDM2B-induced activation of paracrine signaling suggested by this experiment, was further supported by western blot studies showing that the knockdown of KDM2B upregulates tyrosine phosphorylation. Receptor tyrosine kinases that may be activated by shKDM2B, include ERBB2, whose expression and phosphorylation at Y1248, correlates negatively with KDM2B in basal-like breast cancer, and ERBB3, whose expression also

exhibits a negative correlation with KDM2B in the same tumors (Figure S7) (https://www.cbioportal.org).

In summary, data presented in this report identify a novel SLUG turnover paracrine mechanism regulated by KDM2B, with relevant consequences in the differentiation of mammary myoepithelial and basal-like breast cancer cells. KDM2B knockdown destabilized the SLUG protein through convergence of a GSK3 inactivation pathway and a multi-dimensional calpain activation pathway that depends on the upregulation of intracellular Ca2+ and the downregulation of Calpastatin . These data confirm the relevance of KDM2B and GSK3β as potential therapeutic targets in Basal-like breast cancer.

MATERIAL AND METHODS

Cell culture:

Human mammary gland derived cell lines and culture media listed are listed in Table S3. Cells were transduced with packaged lentivirus or γ-retrovirus constructs, using standard procedures. Inhibitors, growth factors and chemicals used for cell culture experiments are detailed in Table S4.

shRNAs and expression vectors. Cloning and site-directed mutagenesis:

Lentiviral shRNA constructs for human KDM2B and calpastatin were purchased from Dharmacon. Expression constructs 3xFLAG-SLUG-WT and 3xFLAG-SLUG-4A (S92A / S96A / S100A / S104A) were a kind gift from Dr. Stephen J. Weiss (Wu et al., 2012). GSK3β (NM_002093.3) with a C-terminal Myc tag was cloned into pLenti-CMV-DEST using the gateway cloning system. KDM2B WT and point and deletion mutants described previously (Pfau et al., 2008), were transferred to the pLX304 lentivirus vector, using the Gateway LR clonase II system (Thermo Fisher Scientific Cat. # 11791020).DNA primers for subcloning and site-directed mutagenesis are listed also in Table S5.

Real time RT-PCR:

cDNA was synthesized using the Retroscript reverse transcription kit (Thermo Fisher Scientific, Cat. #AM1710) and total cell RNA extracted using Tripure (Sigma-Aldrich Cat. #11667157001). Gene expression was quantified by real time RT-PCR, using SYBR Green I master mix (Roche, Cat. #04887352001). The primer sets used for all the real time PCR assays are listed on the Table S7.

Immunoprecipitation and Immunoblotting:

Cells were lysed in Triton X-100 lysis buffer (20 mM Tris (pH 7.5), 150 mM NaCl, 1 mM EDTA, 1 mM EGTA, 1% Triton X-100) supplemented with protease and phosphatase inhibitor cocktails (Sigma-Aldrich, Cat. # 11697498001 and Cat. # 4906837001 respectively). Immunoblotting and immunoprecipitation followed by immunoblotting, were carried out using standard procedures. All antibodies used in the experiments in this report are listed in Table S8.

Intracellular calcium levels

Cells loaded with Fluo3-AM (Molecular probes, Cat. #F1241) were trypsinized and the intensity of fluorescence induced by Ca^{2+} binding was measured by flow cytometry.

Calpain activity assay

Cells were lysed in an EDTA-free lysis buffer containing 20 mM Tris-HCl pH=7.5 and supplemented with a protease inhibitor cocktail (Sigma-Aldrich, Cat. # 4693159001). Calpain activity was measured using the Calpain-Glo assay (Promega, Cat. # G8501)

Calpain-mediated cleavage of SLUG in vitro before and after phosphorylation by GSK3β

3xFlag-SLUG-WT/2A/4A proteins were immunoprecipitated from cells transduced with the corresponding constructs and the immunoprecipitates were phosphorylated by GSK3β in vitro. Following confirmation of the selective phosphorylation of the immunoprecipitated proteins, wild type and mutant proteins were treated similarly with calpain 1 (Sigma-Aldrich, Cat. #C6108) in vitro and their cleavage was assessed by immunoblotting.

Flow cytometry

Following trysinization, 500,000 cells were stained with antibodies specific for phosphor-AKT (Ser473), or cell surface differentiation markers, using standard procedures, and the intensity of staining was measured by flowcytometry.

Statistical analysis

All experiments were performed three times and data are presented as mean ± SD. Two-group comparisons were performed by Student t-test or Mann–Whitney U-test depending on sample distribution. P-values of less than 0.05 were considered significant. Statistical analyses were carried out using Statistical Package for the Social Sciences (SPSS) version 19.0.

ACKOWLEDGMENTS

The authors wish to thank Dr Philip Hinds and Charlotte Kuperwasser (Tufts University School of Medicine) and all the members of the Tsichlis lab for helpful discussions. This work was supported by the NIH grant R01 CA109747 and by start-up funds from the OSUCCC to P.N. Tsichlis. Elia Aguado Fraile was supported by a postdoctoral fellowship from the Alfonso Martin Escudero Foundation (Spain). Georgios I. Laliotis is supported by the Pelotonia Post-Doctoral fellowship from OSUCCC.

REFERENCES

Andricovich, J., Kai, Y., Peng, W., Foudi, A., and Tzatsos, A. (2016). Histone demethylase KDM2B regulates lineage commitment in normal and malignant hematopoiesis. J Clin Invest *126*, 905-920.

Barrero, M.J., and Izpisua Belmonte, J.C. (2013). Polycomb complex recruitment in pluripotent stem cells. Nat Cell Biol *15*, 348-350.

Boulard, M., Edwards, J.R., and Bestor, T.H. (2015). FBXL10 protects Polycomb-bound genes from hypermethylation. Nat Genet *47*, 479-485.

Davies, B.R., Greenwood, H., Dudley, P., Crafter, C., Yu, D.H., Zhang, J., Li, J., Gao, B., Ji, Q., Maynard, J.*, et al.* (2012). Preclinical pharmacology of AZD5363, an inhibitor of AKT: pharmacodynamics, antitumor activity, and correlation of monotherapy activity with genetic background. Mol Cancer Ther *11*, 873-887.

De Tullio, R., Averna, M., Salamino, F., Pontremoli, S., and Melloni, E. (2000). Differential degradation of calpastatin by mu- and m-calpain in Ca(2+)-enriched human neuroblastoma LAN-5 cells. FEBS Lett *475*, 17-21.

Denkert, C., Liedtke, C., Tutt, A., and von Minckwitz, G. (2017). Molecular alterations in triple-negative breast cancer-the road to new treatment strategies. Lancet *389*, 2430-2442.

Dikic, I., and Elazar, Z. (2018). Mechanism and medical implications of mammalian autophagy. Nat Rev Mol Cell Biol *19*, 349-364.

Gao, R., Dong, R., Du, J., Ma, P., Wang, S., and Fan, Z. (2013). Depletion of histone demethylase KDM2A inhibited cell proliferation of stem cells from apical papilla by de-repression of p15INK4B and p27Kip1. Mol Cell Biochem *379*, 115-122.

Gasser, J.A., Inuzuka, H., Lau, A.W., Wei, W., Beroukhim, R., and Toker, A. (2014). SGK3 mediates INPP4B-dependent PI3K signaling in breast cancer. Mol Cell *56*, 595-607.

Gewinner, C., Wang, Z.C., Richardson, A., Teruya-Feldstein, J., Etemadmoghadam, D., Bowtell, D., Barretina, J., Lin, W.M., Rameh, L., Salmena, L.*, et al.* (2009). Evidence that inositol polyphosphate 4-phosphatase type II is a tumor suppressor that inhibits PI3K signaling. Cancer Cell *16*, 115-125.

Gray, J.E., Infante, J.R., Brail, L.H., Simon, G.R., Cooksey, J.F., Jones, S.F., Farrington, D.L., Yeo, A., Jackson, K.A., Chow, K.H.*, et al.* (2015). A first-in-human phase I dose-escalation, pharmacokinetic, and pharmacodynamic evaluation of intravenous LY2090314, a glycogen synthase kinase 3 inhibitor, administered in combination with pemetrexed and carboplatin. Invest New Drugs *33*, 1187-1196.

Guo, W., Keckesova, Z., Donaher, J.L., Shibue, T., Tischler, V., Reinhardt, F., Itzkovitz, S., Noske, A., Zurrer-Hardi, U., Bell, G.*, et al.* (2012). Slug and Sox9 cooperatively determine the mammary stem cell state. Cell *148*, 1015-1028.

He, J., Kallin, E.M., Tsukada, Y., and Zhang, Y. (2008). The H3K36 demethylase Jhdm1b/Kdm2b regulates cell proliferation and senescence through p15(Ink4b). Nat Struct Mol Biol *15*, 1169-1175.

Kalimutho, M., Parsons, K., Mittal, D., Lopez, J.A., Srihari, S., and Khanna, K.K. (2015). Targeted Therapies for Triple-Negative Breast Cancer: Combating a Stubborn Disease. Trends Pharmacol Sci *36*, 822-846.

Kamei, H., Saito, T., Ozawa, M., Fujita, Y., Asada, A., Bibb, J.A., Saido, T.C., Sorimachi, H., and Hisanaga, S. (2007). Suppression of calpain-dependent cleavage of the CDK5 activator p35 to p25 by site-specific phosphorylation. J Biol Chem *282*, 1687-1694.

Kampranis, S.C., and Tsichlis, P.N. (2009). Histone demethylases and cancer. Adv Cancer Res *102*, 103-169.

Kang, J.Y., Kim, J.Y., Kim, K.B., Park, J.W., Cho, H., Hahm, J.Y., Chae, Y.C., Kim, D., Kook, H., Rhee, S.*, et al.* (2018). KDM2B is a histone H3K79 demethylase and induces transcriptional repression via sirtuin-1-mediated chromatin silencing. Faseb j *32*, 5737-5750.

Kao, S.H., Wang, W.L., Chen, C.Y., Chang, Y.L., Wu, Y.Y., Wang, Y.T., Wang, S.P., Nesvizhskii, A.I., Chen, Y.J., Hong, T.M.*, et al.* (2014). GSK3beta controls epithelial-mesenchymal transition and tumor metastasis by CHIP-mediated degradation of Slug. Oncogene *33*, 3172-3182.

Kelsey, G. (2015). Keeping methylation at bay. Nat Genet *47*, 427-428.

Kiely, M., and Kiely, P.A. (2015). PP2A: The Wolf in Sheep's Clothing? Cancers (Basel) *7*, 648-669.

Kim, J.T., Kim, J.W., Kang, Y.H., Kim, K.D., Lee, S.J., Choi, S.C., Kim, K.S., Chae, S.K., Kim, J.W., Lim, J.S.*, et al.* (2012). NDRG2 and PRA1 interact and synergistically inhibit T-cell factor/beta-catenin signaling. FEBS Lett *586*, 3962-3968.

Konuma, T., Nakamura, S., Miyagi, S., Negishi, M., Chiba, T., Oguro, H., Yuan, J., Mochizuki-Kashio, M., Ichikawa, H., Miyoshi, H.*, et al.* (2011). Forced expression of the histone demethylase Fbxl10 maintains self-renewing hematopoietic stem cells. Exp Hematol *39*, 697-709.e695.

Kottakis, F., Foltopoulou, P., Sanidas, I., Keller, P., Wronski, A., Dake, B.T., Ezell, S.A., Shen, Z., Naber, S.P., Hinds, P.W.*, et al.* (2014). NDY1/KDM2B functions as a master regulator of polycomb complexes and controls self-renewal of breast cancer stem cells. Cancer Res *74*, 3935-3946.

Kottakis, F., Polytarchou, C., Foltopoulou, P., Sanidas, I., Kampranis, S.C., and Tsichlis, P.N. (2011). FGF-2 regulates cell proliferation, migration, and angiogenesis through an NDY1/KDM2B-miR-101-EZH2 pathway. Mol Cell *43*, 285-298.

Lagarou, A., Mohd-Sarip, A., Moshkin, Y.M., Chalkley, G.E., Bezstarosti, K., Demmers, J.A., and Verrijzer, C.P. (2008). dKDM2 couples histone H2A ubiquitylation to histone H3 demethylation during Polycomb group silencing. Genes Dev *22*, 2799-2810.

Lee, H., and Ro, J.Y. (2015). Differential expression of GSK3beta and pS9GSK3beta in normal human tissues: can pS9GSK3beta be an epithelial marker? Int J Clin Exp Pathol *8*, 4064-4073.

Li Chew, C., Lunardi, A., Gulluni, F., Ruan, D.T., Chen, M., Salmena, L., Nishino, M., Papa, A., Ng, C., Fung, J.*, et al.* (2015). In Vivo Role of INPP4B in Tumor and Metastasis Suppression through Regulation of PI3K-AKT Signaling at Endosomes. Cancer Discov *5*, 740-751.

Liang, G., He, J., and Zhang, Y. (2012). Kdm2b promotes induced pluripotent stem cell generation by facilitating gene activation early in reprogramming. Nat Cell Biol *14*, 457-466.

Lopez-Menendez, C., Gamir-Morralla, A., Jurado-Arjona, J., Higuero, A.M., Campanero, M.R., Ferrer, I., Hernandez, F., Avila, J., Diaz-Guerra, M., and Iglesias, T. (2013). Kidins220 accumulates with tau in human Alzheimer's disease and related models: modulation of its calpain-processing by GSK3beta/PP1 imbalance. Hum Mol Genet *22*, 466-482.

Ma, S., Liu, S., Huang, Q., Xie, B., Lai, B., Wang, C., Song, B., and Li, M. (2012). Site-specific phosphorylation protects glycogen synthase kinase-3beta from calpain-mediated truncation of its N and C termini. J Biol Chem *287*, 22521-22532.

McCubrey, J.A., Steelman, L.S., Bertrand, F.E., Davis, N.M., Sokolosky, M., Abrams, S.L., Montalto, G., D'Assoro, A.B., Libra, M., Nicoletti, F.*, et al.* (2014). GSK-3 as potential target for therapeutic intervention in cancer. Oncotarget *5*, 2881-2911.

McKenna, J.P., and Hanson, P.J. (1993). Inhibition by Ro 31-8220 of acid secretory activity induced by carbachol indicates a stimulatory role for protein kinase C in the action of muscarinic agonists on isolated rat parietal cells. Biochem Pharmacol *46*, 583-588.

McNiel, E.A., and Tsichlis, P.N. (2017). Analyses of publicly available genomics resources define FGF-2-expressing bladder carcinomas as EMT-prone, proliferative tumors with low mutation rates and high expression of CTLA-4, PD-1 and PD-L1. Signal Transduct Target Ther *2*.

Mertins, P., Mani, D.R., Ruggles, K.V., Gillette, M.A., Clauser, K.R., Wang, P., Wang, X., Qiao, J.W., Cao, S., Petralia, F.*, et al.* (2016). Proteogenomics connects somatic mutations to signalling in breast cancer. Nature *534*, 55-62.

Mizushima, N., Yoshimori, T., and Levine, B. (2010). Methods in mammalian autophagy research. Cell *140*, 313-326.

Monteverde, T., Tait-Mulder, J., Hedley, A., Knight, J.R., Sansom, O.J., and Murphy, D.J. (2018). Calcium signalling links MYC to NUAK1. Oncogene *37*, 982-992.

Nagy, A., Lanczky, A., Menyhart, O., and Gyorffy, B. (2018). Validation of miRNA prognostic power in hepatocellular carcinoma using expression data of independent datasets. Sci Rep *8*, 9227.

Pearce, L.R., Alton, G.R., Richter, D.T., Kath, J.C., Lingardo, L., Chapman, J., Hwang, C., and Alessi, D.R. (2010). Characterization of PF-4708671, a novel and highly specific inhibitor of p70 ribosomal S6 kinase (S6K1). Biochem J *431*, 245-255.

Peti, W., Nairn, A.C., and Page, R. (2013). Structural basis for protein phosphatase 1 regulation and specificity. Febs j *280*, 596-611.

Pfau, R., Tzatsos, A., Kampranis, S.C., Serebrennikova, O.B., Bear, S.E., and Tsichlis, P.N. (2008). Members of a family of JmjC domain-containing oncoproteins immortalize embryonic fibroblasts via a JmjC domain-dependent process. Proc Natl Acad Sci U S A *105*, 1907-1912.

Polytarchou, C., Pfau, R., Hatziapostolou, M., and Tsichlis, P.N. (2008). The JmjC domain histone demethylase Ndy1 regulates redox homeostasis and protects cells from oxidative stress. Mol Cell Biol *28*, 7451-7464.

Prat, A., Adamo, B., Cheang, M.C., Anders, C.K., Carey, L.A., and Perou, C.M. (2013). Molecular characterization of basal-like and non-basal-like triple-negative breast cancer. Oncologist *18*, 123-133.

Prat, A., Ellis, M.J., and Perou, C.M. (2011). Practical implications of gene-expression-based assays for breast oncologists. Nat Rev Clin Oncol *9*, 48-57.

Proia, T.A., Keller, P.J., Gupta, P.B., Klebba, I., Jones, A.D., Sedic, M., Gilmore, H., Tung, N., Naber, S.P., Schnitt, S.*, et al.* (2011). Genetic predisposition directs breast cancer phenotype by dictating progenitor cell fate. Cell Stem Cell *8*, 149-163.

Putney, J.W., Steinckwich-Besancon, N., Numaga-Tomita, T., Davis, F.M., Desai, P.N., D'Agostin, D.M., Wu, S., and Bird, G.S. (2017). The functions of store-operated calcium channels. Biochim Biophys Acta Mol Cell Res *1864*, 900-906.

Qu, Y., Han, B., Yu, Y., Yao, W., Bose, S., Karlan, B.Y., Giuliano, A.E., and Cui, X. (2015). Evaluation of MCF10A as a Reliable Model for Normal Human Mammary Epithelial Cells. PLoS One *10*, e0131285.

Sapkota, G.P., Cummings, L., Newell, F.S., Armstrong, C., Bain, J., Frodin, M., Grauert, M., Hoffmann, M., Schnapp, G., Steegmaier, M.*, et al.* (2007). BI-D1870 is a specific inhibitor of the p90 RSK (ribosomal S6 kinase) isoforms in vitro and in vivo. Biochem J *401*, 29-38.

Sarrio, D., Rodriguez-Pinilla, S.M., Hardisson, D., Cano, A., Moreno-Bueno, G., and Palacios, J. (2008). Epithelial-mesenchymal transition in breast cancer relates to the basal-like phenotype. Cancer Res *68*, 989-997.

Sherk, A.B., Frigo, D.E., Schnackenberg, C.G., Bray, J.D., Laping, N.J., Trizna, W., Hammond, M., Patterson, J.R., Thompson, S.K., Kazmin, D.*, et al.* (2008). Development of a small-molecule serum- and glucocorticoid-regulated kinase-1 antagonist and its evaluation as a prostate cancer therapeutic. Cancer Res *68*, 7475-7483.

Skibinski, A., Breindel, J.L., Prat, A., Galvan, P., Smith, E., Rolfs, A., Gupta, P.B., LaBaer, J., and Kuperwasser, C. (2014). The Hippo transducer TAZ interacts with the SWI/SNF complex to regulate breast epithelial lineage commitment. Cell Rep *6*, 1059-1072.

Spike, B.T., Engle, D.D., Lin, J.C., Cheung, S.K., La, J., and Wahl, G.M. (2012). A mammary stem cell population identified and characterized in late embryogenesis reveals similarities to human breast cancer. Cell Stem Cell *10*, 183-197.

Storr, S.J., Mohammed, R.A., Woolston, C.M., Green, A.R., Parr, T., Spiteri, I., Caldas, C., Ball, G.R., Ellis, I.O., and Martin, S.G. (2011a). Calpastatin is associated with lymphovascular invasion in breast cancer. Breast *20*, 413-418.

Storr, S.J., Woolston, C.M., Barros, F.F., Green, A.R., Shehata, M., Chan, S.Y., Ellis, I.O., and Martin, S.G. (2011b). Calpain-1 expression is associated with relapse-free survival in breast cancer patients treated with trastuzumab following adjuvant chemotherapy. Int J Cancer *129*, 1773-1780.

Tsukada, Y., Fang, J., Erdjument-Bromage, H., Warren, M.E., Borchers, C.H., Tempst, P., and Zhang, Y. (2006). Histone demethylation by a family of JmjC domain-containing proteins. Nature *439*, 811-816.

Tzatsos, A., Paskaleva, P., Ferrari, F., Deshpande, V., Stoykova, S., Contino, G., Wong, K.K., Lan, F., Trojer, P., Park, P.J.*, et al.* (2013). KDM2B promotes pancreatic cancer via Polycomb-dependent and -independent transcriptional programs. J Clin Invest *123*, 727-739.

Tzatsos, A., Pfau, R., Kampranis, S.C., and Tsichlis, P.N. (2009). Ndy1/KDM2B immortalizes mouse embryonic fibroblasts by repressing the Ink4a/Arf locus. Proc Natl Acad Sci U S A *106*, 2641-2646.

van den Boom, V., Maat, H., Geugien, M., Rodriguez Lopez, A., Sotoca, A.M., Jaques, J., Brouwers-Vos, A.Z., Fusetti, F., Groen, R.W., Yuan, H.*, et al.* (2016). Non-canonical PRC1.1 Targets Active Genes Independent of H3K27me3 and Is Essential for Leukemogenesis. Cell Rep *14*, 332-346.

Vijay, G.V., Zhao, N., Den Hollander, P., Toneff, M.J., Joseph, R., Pietila, M., Taube, J.H., Sarkar, T.R., Ramirez-Pena, E., Werden, S.J.*, et al.* (2019). GSK3beta regulates epithelial-mesenchymal transition and cancer stem cell properties in triple-negative breast cancer. Breast Cancer Res *21*, 37.

Wang, J.J., Dong, R., Wang, L.P., Wang, J.S., Du, J., Wang, S.L., Shan, Z.C., and Fan, Z.P. (2015). Histone demethylase KDM2B inhibits the chondrogenic differentiation potentials of stem cells from apical papilla. Int J Clin Exp Med *8*, 2165-2173.

Wang, T., Chen, K., Zeng, X., Yang, J., Wu, Y., Shi, X., Qin, B., Zeng, L., Esteban, M.A., Pan, G.*, et al.* (2011). The histone demethylases Jhdm1a/1b enhance somatic cell reprogramming in a vitamin-C-dependent manner. Cell Stem Cell *9*, 575-587.

Wang, Y., Zang, J., Zhang, D., Sun, Z., Qiu, B., and Wang, X. (2018). KDM2B overexpression correlates with poor prognosis and regulates glioma cell growth. Onco Targets Ther *11*, 201-209.

Wendt, A., Thompson, V.F., and Goll, D.E. (2004). Interaction of calpastatin with calpain: a review. Biol Chem *385*, 465-472.

Wu, Z.Q., Li, X.Y., Hu, C.Y., Ford, M., Kleer, C.G., and Weiss, S.J. (2012). Canonical Wnt signaling regulates Slug activity and links epithelial-mesenchymal transition with epigenetic Breast Cancer 1, Early Onset (BRCA1) repression. Proc Natl Acad Sci U S A *109*, 16654-16659.

Xu, C., Kim, N.G., and Gumbiner, B.M. (2009). Regulation of protein stability by GSK3 mediated phosphorylation. Cell Cycle *8*, 4032-4039.

Yu, X., Wang, J., Wu, J., and Shi, Y. (2015). A systematic study of the cellular metabolic regulation of Jhdm1b in tumor cells. Mol Biosyst *11*, 1867-1875.

Yuen, E.Y., Liu, W., and Yan, Z. (2007). The phosphorylation state of GluR1 subunits determines the susceptibility of AMPA receptors to calpain cleavage. J Biol Chem *282*, 16434-16440.

Zacharopoulou, N., Tsapara, A., Kallergi, G., Schmid, E., Alkahtani, S., Alarifi, S., Tsichlis, P.N., Kampranis, S.C., and Stournaras, C. (2018). The Epigenetic Factor KDM2B Regulates EMT and Small GTPases in Colon Tumor Cells. Cell Physiol Biochem *47*, 368-377.

Zakikhan, K., Pournasr, B., Nassiri-Asl, M., and Baharvand, H. (2016). Enhanced direct conversion of fibroblasts into hepatocyte-like cells by Kdm2b. Biochem Biophys Res Commun *474*, 97-103.

FIGURES

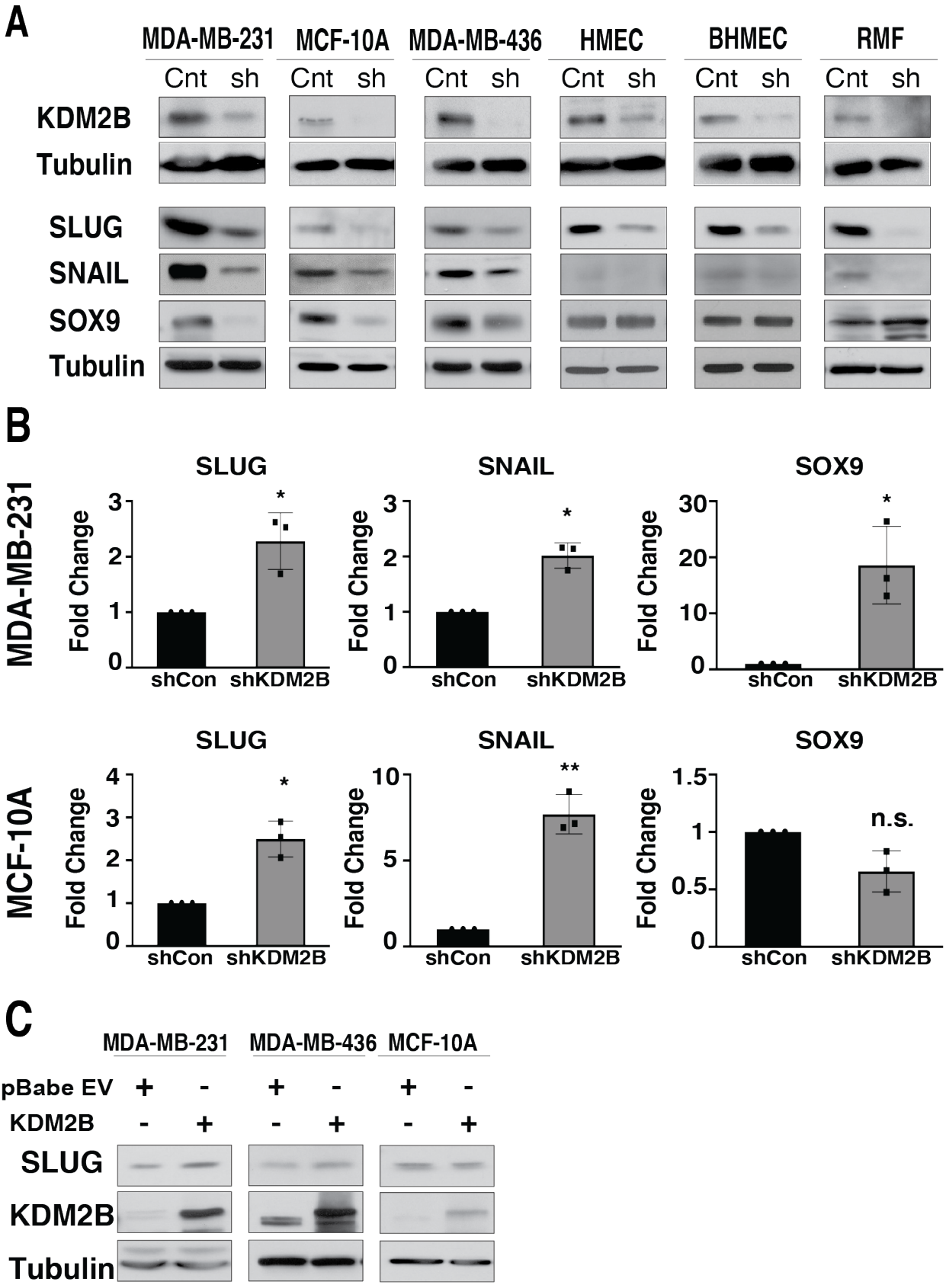
A
MDA-MB-231
MCF-10A
MDA-MB-436
HMEC
BHMEC
RMF
Cnt sh
KDM2B
Tubulin
SLUG
SNAIL
SOX9
Tubulin
B
MDA-MB-231
MCF-10A
SLUG
SNAIL
SOX9
Fold Change
shCon
shKDM2B
n.s.
C
MDA-MB-231
MDA-MB-436
MCF-10A
pBabe EV
KDM2B
SLUG
KDM2B
Tubulin

Figure 1: KDM2B regulates the expression of SLUG, SNAIL and SOX9 postranscriptionally: ***A.*** Immunoblotting of cell lysates of a panel of human mammary gland-derived cell lines transduced with shControl (Cntrl) or shKDM2B (sh) lentiviral constructs, shows that the knockdown of KDM2B results in the downregulation of SLUG, SNAIL and SOX9. **B.** Quantitative RT-PCR failed to detect downregulation of SLUG, SNAIL and SOX9 in shKDM2B-transduced MDA-MB-231 and MCF10A cells. qRT-PCR of RNA from the remaining cell lines (MDA-MB-436, HMEC, BHMEC and RMF) gave similar results (Fig S1A). **C.** Western blots of control (Cntrl) and KDM2B-overexpressing MDA-MB-231, MDA-MB-436 and MCF-10A cells revealed upregulation of SLUG in MDA-MB-231 and MDA-MB-436, but not in MCF-10A cells.

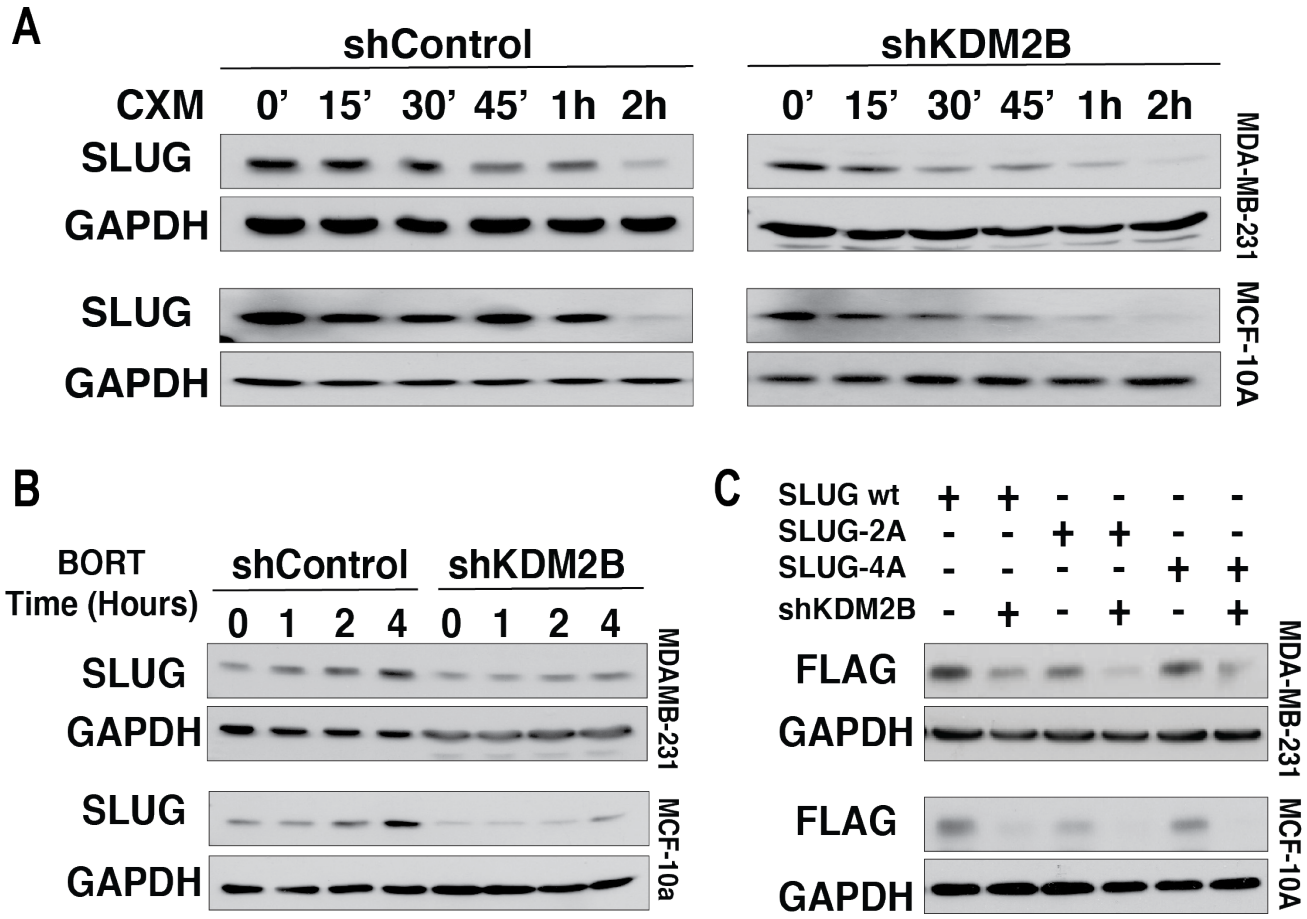

Figure 2: shKDM2B destabilizes SLUG by a proteasome-independent mechanism: A. shCntrl (Left panel) and shKDM2B-transduced (Right panel) MDA-MB-231 and MCF-10A cells were treated with Cycloheximide (CHX) (30 µg/ml) and they were harvested at sequential time points, as indicated. Probing western blots of the harvested cell lysates with anti-SLUG or anti-GAPDH

(loading control) antibodies, showed that the degradation of SLUG was more rapid in the shKDM2B cells. **B.** shCntrl and shKDM2B-transduced MDA-MB-231 and MCF-10A cells were treated with the proteasome inhibitor Bortezomib (BORT) (0.5 μM) and they were harvested at sequential time points, as indicated. Probing western blots of the harvested cell lysates with anti-SLUG or anti-GAPDH (loading control) antibodies, showed a more robust upregulation in the shCntrl than in the ShKDM2B-transduced cells, suggesting that the destabilization of SLUG by shKDM2B is proteasome independent. **C.** shCntrl and shKDM2B-transduced MDA-MB-231 and MCF10A cells were rescued with SLUG-WT, SLUG2A and SLUG-4A lentiviral constructs. Probing western blots of lysates derived from these cells with anti-SLUG or anti-GAPDH (loading control) antibodies, showed that neither the wild type nor the mutant SLUG proteins rescue the shKDM2B-induced downregulation of SLUG. Given that shKDM2B downregulates SLUG, the loading in panels A and B was adjusted so that the amount of SLUG protein before the start of the treatment would be similar

in the shCntrl and shKDM2B cells.

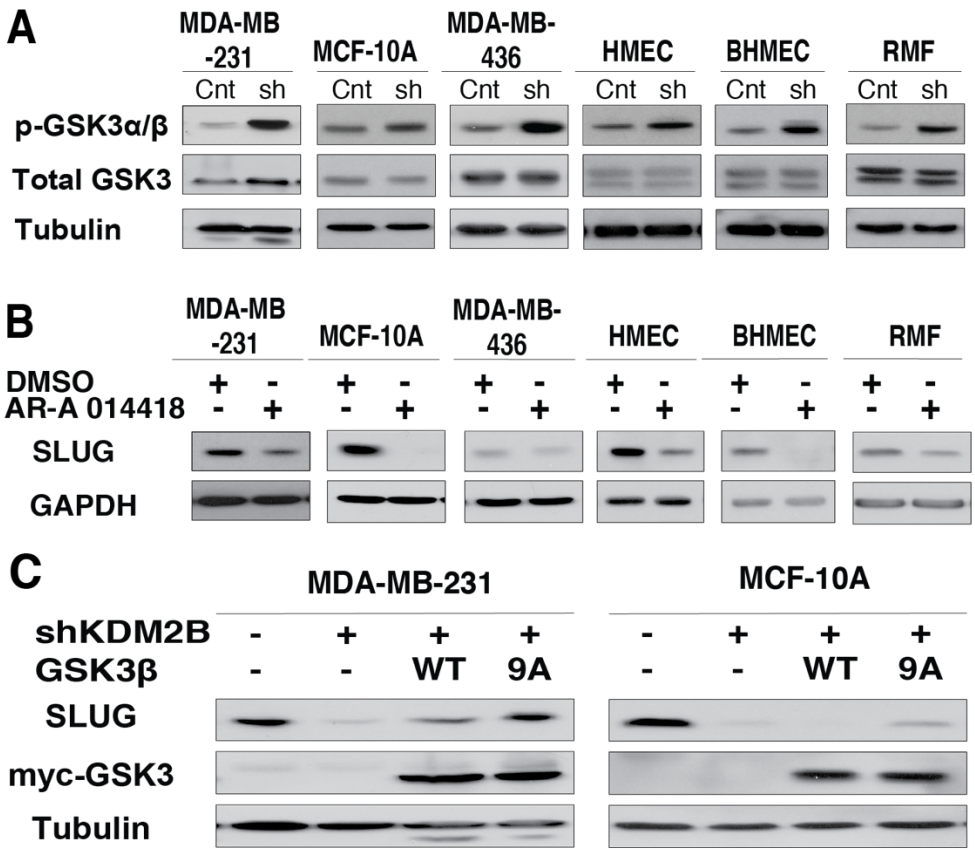

Figure 3: The knockdown of KDM2B destabilizes SLUG, in part by promoting the inhibitory phosphorylation of GSK3β at Ser9. A. The six human mammary gland-derived cell lines in our panel, were transduced with shControl (Cntrl) or shKDM2B (sh) lentiviral constructs. Probing immunoblots of cell lysates from these cell lines with anti-GSK3α/β anti-Total GSK3 and anti-Tubulin (loading control) antibodies, revealed that shKDM2B promotes GSK3 phosphorylation. **B.** The six human mammary gland-derived cell lines in our panel were treated with the GSK3 inhibitor AR-A 014418 (2 μM), or DMSO for 48 hours. Probing immunoblots of cell lysates from these cell lines with anti-SLUG or anti-GAPDH (loading control) antibodies, revealed that the inhibition of GSK3 results in the downregulation of SLUG. **C.** MDA-MB-231 cells (Left panel) and MCF-10A cells (Right panel), transduced with shCntrl or shKDM2B lentiviral constructs, were rescued with wild type GSK3β, or the constitutively-active GSK3β S9A mutant. Probing immunoblots of lysates derived from these cells

with the indicated antibodies, showed that the GSK3β S9A mutant rescues the SLUG downregulation fully in MDA-MB-231 cells and partially in MCF-10A cells.

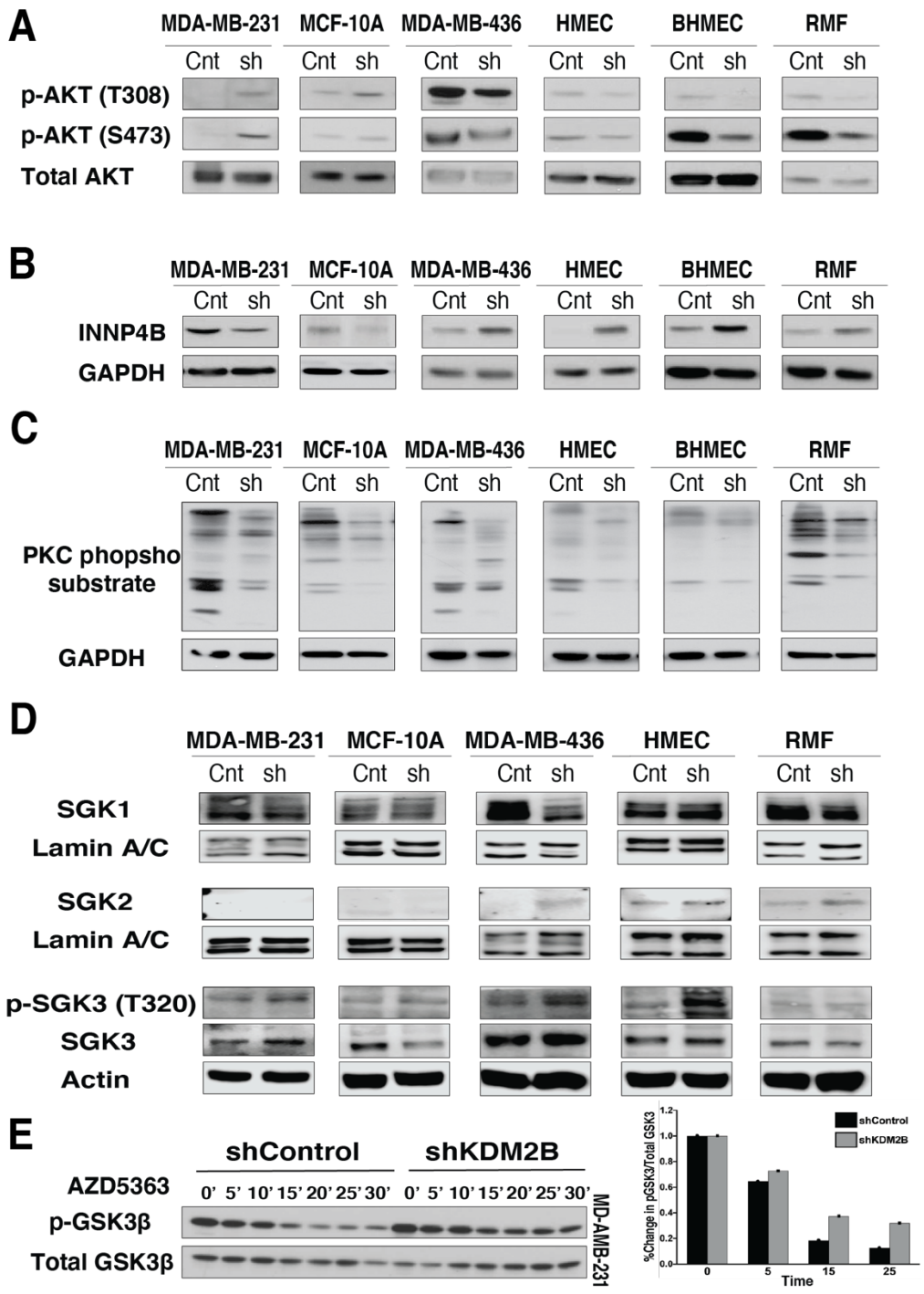

Figure 4: KDM2B knockdown enhances the phosphorylation of GSK3β, by inhibiting its dephosphorylation: A. The six cell lines in our mammary cell line panel were transduced with shCntrl or shKDM2B lentiviral constructs. Probing immunoblots of cell lysates of these cell lines with anti-phospho-AKT (Thr308 and Ser473) and anti-Total AKT antibodies, revealed that shKDM2B promotes

AKT activation in some cell lines (MDA-MB-231 and MCF-10A) and deactivation in others (MDA-MB-436, HMEC, BHMEC and RMF). **B.** Probing immunoblots of the same lysates with anti-INPP4B and anti-GAPDH (loading control) antibodies, revealed that the expression of INPP4B exhibits a perfect negative correlation with the phosphorylation of AKT. **C.** Probing immunoblots of the same lysates with a classical PKC phospho-substrate antibody, revealed that PKC is inhibited in shKDM2B-transduced cells. **D.** Probing immunoblots of cell lysates from five of the cell lines in our cell line panel, with anti-SGK1, anti-SGK2, anti-SGK3, and anti-phospho-SGK3 antibodies, shows that shKDM2B promotes the upregulation of SGK2 in in three cell lines and the phosphorylation of SGK3 in two. **E.** MDA-MB-231 cells were treated with the pan-AKT inhibitor AZD-5363 (5 μM) and they were lysed and harvested at the indicated time points. Probing immunoblots of these lysates with anti-phospho-GSK3β and anti-Total GSK3β antibodies, revealed that shKDM2B stabilizes GSK3β phosphorylation.

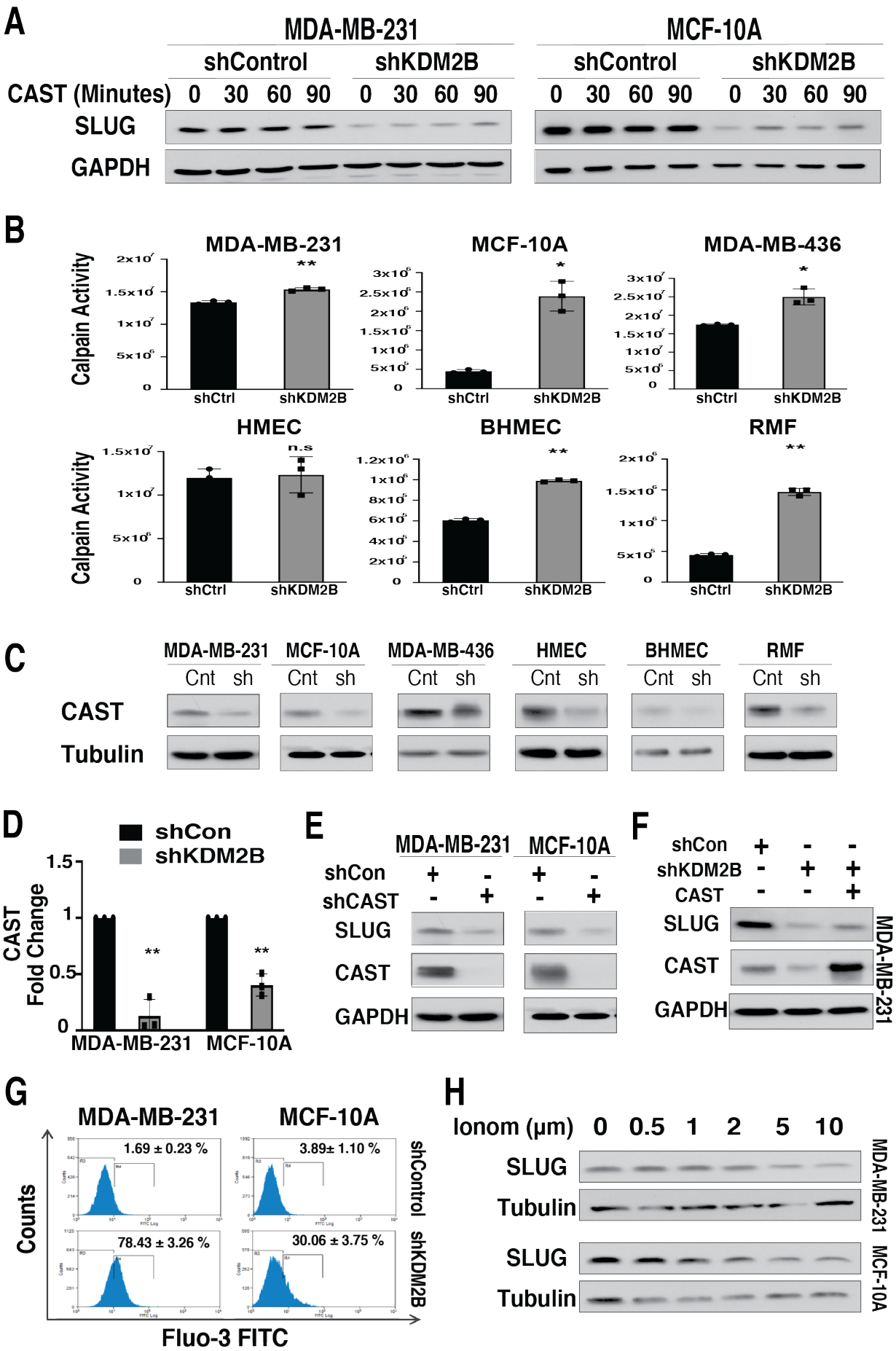
A
MDA-MB-231
MCF-10A
shControl
shKDM2B
CAST (Minutes) 0 30 60 90 0 30 60 90
SLUG
GAPDH
B
MDA-MB-231
MCF-10A
MDA-MB-436
HMEC
BHMEC
RMF
Calpain Activity
shCtrl
shKDM2B
n.s
C
MDA-MB-231 MCF-10A MDA-MB-436 HMEC BHMEC RMF
Cnt sh
CAST
Tubulin
D
shCon
shKDM2B
CAST Fold Change
MDA-MB-231 MCF-10A
E
MDA-MB-231 MCF-10A
shCon
shCAST
SLUG
CAST
GAPDH
F
shCon
shKDM2B
CAST
SLUG
CAST
GAPDH
MDA-MB-231
G
MDA-MB-231
MCF-10A
1.69 ± 0.23 %
3.89± 1.10 %
78.43 ± 3.26 %
30.06 ± 3.75 %
shControl
shKDM2B
Counts
Fluo-3 FITC
H
Ionom (μm) 0 0.5 1 2 5 10
SLUG
Tubulin
MDA-MB-231
MCF-10A

Figure 5: KDM2B knockdown promotes calpain-mediated degradation of SLUG: **A.** MDA-MB-231 cells (Left panel) and MCF-10A cells (Right panel), transduced with shCntrl or shKDM2B lentiviral constructs, were treated with a cell permeable peptide derived from calpastatin (CAST), an inhibitor of calpains 1, 2, and 9, and they were lysed and harvested at sequential time points, as indicated. Probing western blots of the harvested cell lysates with anti-SLUG or anti-GAPDH (loading control) antibodies, showed upregulation of SLUG only in the shKDM2B-transduced cells, suggesting that the destabilization of SLUG by shKDM2B depends on the activation of calpains 1, 2 or 9 **B.** Measurement of the activity of calpains 1 and 2, using a luminescent assay in all six mammary cell lines in our panel, following transduction with shCntrl and shKDM2B constructs, confirmed the activation of these calpains by shKDM2B. Data are presented as mean ± SD of three independent experiments and asterisks indicate statistical significance (* p-value ≤ 0.05, ** p-value ≤ 0.01, *** p-value ≤ 0.001). **C.** Probing immunoblots of cell lysates from the cell lines in B with an anti-calpastatin antibody revealed a robust downregulation of calpastain in all the shKDM2B-transduced cell lines. **D.** Measurement of the calpastatin mRNA levels by quantitative RT-PCR in shCntrl and shKDM2B-transduced MDA-MB-231 and MCF10A cells, revealed that calpastatin is downregulated by KDM2B at the RNA level. **E.** Probing immunoblots of shCntrl and shCAST (Calpastatin)-transduced MDA-MB-231 and MCF10A cells with the indicated antibodies, revealed that the knockdown of calpastatin is sufficient to downregulate SLUG. **F.** shKDM2B-transduced MDA-MB-231 cells were rescued with calpastatin or the empty vector (EV) control. Probing immunoblots of lysates from these cells with the indicated antibodies, revealed that calpastatin rescues partially the downregulation of SLUG by shKDM2B. **G.** Fluo-3 staining and flow cytometry of the cells in D, revealed that shKDM2B increases the levels of intracellular Ca^{2+}. **H.** MDA-MB-231 and MCF-10A cells were treated with ionomycin and they were lysed and harvested at the indicated time points. Probing immunoblots of these lysates with anti-SLUG and anti-Tubulin (loading control) antibodies, revealed that SLUG is downregulated rapidly in response to ionomycin treatment.

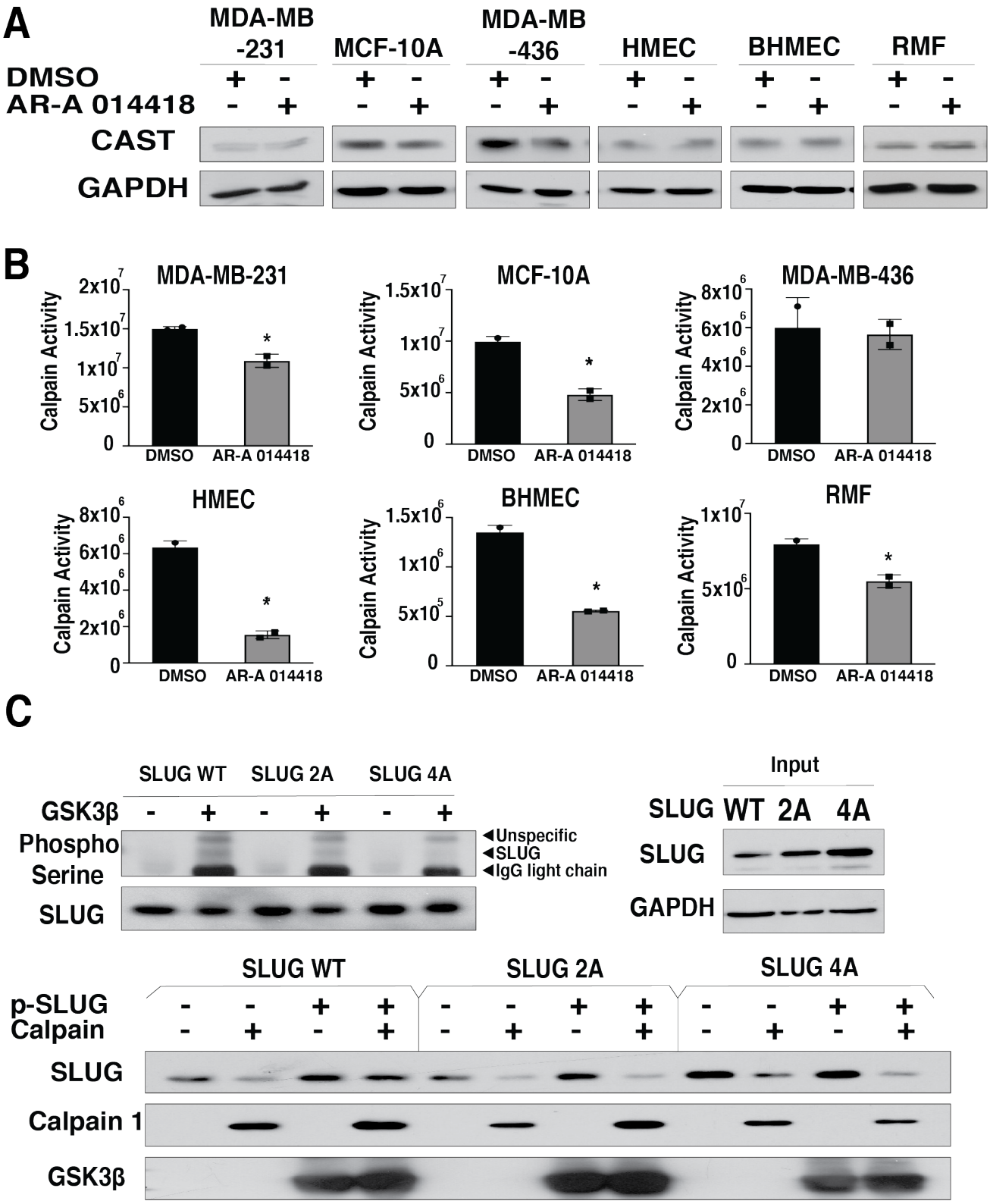

Figure 6: Phosphorylation by GSK3β protects SLUG from calpain degradation. A. The six human mammary gland-derived cell lines in our panel were treated with the GSK3 inhibitor AR-A 014418 (2 μM), or DMSO for 48 hours. Probing immunoblots of cell lysates from these cell lines with

anti-CAST (calpastatin) or anti-GAPDH (loading control) antibodies, revealed that the inhibition of GSK3 results in weak downregulation of Calpastatin in some, but not all the cell lines. **B.** Measurement of the activity of calpains 1 and 2 by a luminescent assay in all six mammary cell lines in panel A, revealed that shKDM2B promotes the inhibition, rather than the activation of these calpains. Data are presented as mean ± SD of three independent experiments and asterisks indicate statistical significance (* p-value ≤ 0.05, ** p-value ≤ 0.01, *** p-value ≤ 0.001). **C** *(Upper panel)* Wild type SLUG (SLUG-WT) and the mutants SLUG-2A and SLUG-4A were expressed and purified from E Coli. The purified proteins were phosphorylated by GSK3β in vitro. Probing an immunoblot of the GSK3β-phosphorylated and the mock-phosphorylated proteins with an anti-phospho-serine antibody (Left upper panel) confirmed the phosphorylation. An immunoblot showing the relative input of SLUG in the phosphorylation reaction is shown in the Right upper panel. *(Lower panel)* In Vitro degradation of phosphorylated and mock phosphorylated SLUG proteins (wild type and mutants) following treatment with purified calpain 1. Immunoblots of the products of the in vitro degradation reaction were probed with anti-SLUG, anti-calpain-1 and anti-GSK3β antibodies.

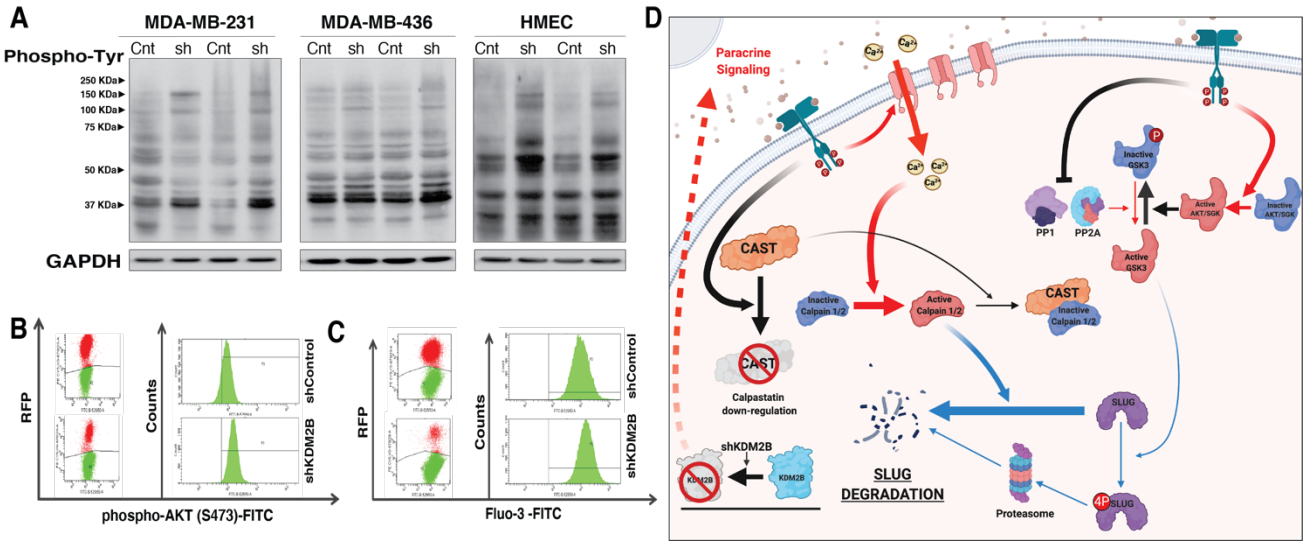

Figure 7: The knockdown of KDM2B in human mammary gland-derived cell lines activates GSK3β phosphorylation and calpain activation pathways via paracrine mechanisms. A. Probing immunoblots of MDA-MB-231, MDA-MB-436 and HMEC cells transdiced with shCntrl or shKDM2B constructs with an antiphosphotyrosine antibody, revealed that shKDM2B promotes an increase in the abundance of tyrosine phosphorylated proteins. **B.** MDA-MB-231 cells engineered to

stably express RFP, from a retrovirus construct, were transduced with shCntrl or shKDM2B constructs. The shCntrl and shKDM2B RFP-positive cells were cocultivated with RFP-negative parental MDA-MB231 cells. Following co-cultivation, the cells were stained with an FITC-labeled anti phosphor-AKT (Ser473) antibody and they were analyzed by flow-cytometry. **C.** Alternatively, the co-cultures were treated with the fluorescent Ca^{2+} indicator FLUO-3 AM and they were also analyzed by flow-cytometry (Right panel). Gating on the RFP-negative cells revealed that they underwent shifts in the abundance of phosphor-AKT and Ca^{2+},when co-cultivated with shKDM2B cells, despite the fact that they were themselves, shKDM2B-negative. **D.** Model of the calpain-dependent degradation of SLUG induced by the knockdown of KDM2B. The knockdown of KDM2B results in the indirect activation of tyrosine kinase receptor-dependent paracrine mechanisms. The tyrosine kinase receptor-initiated signals activate AKT and/or SGK, which phosphorylate GSK3 at Ser9/21. In addition, they block the activities of PP1 and PP2A toward GSK3, phosphorylated at Ser9/21. The ultimate output of these two pathways converging on GSK3 is the enhanced phosphorylation of GSK3 at Ser9/21. The tyrosine kinase receptor signals also induce Ca2+ influx and calpastatin (CAST) downregulation and the combination of these two events results in the activation of calpains 1 and 2. Under steady state conditions, SLUG is phosphorylated by GSK3 and the phosphorylated SLUG undergoes degradation via the proteasome. Inactivation of GSK3 by phosphorylation at Ser9/21 induced by the knockdown of KDM2B, prevents the slow proteasomal degradation of SLUG, but renders SLUG sensitive to degradation by calpains 1 and 2. This results in a switch from the slow proteasomal degradation to the rapid calpain-dependent degradation.

SUPPLEMENTARY FIGURES

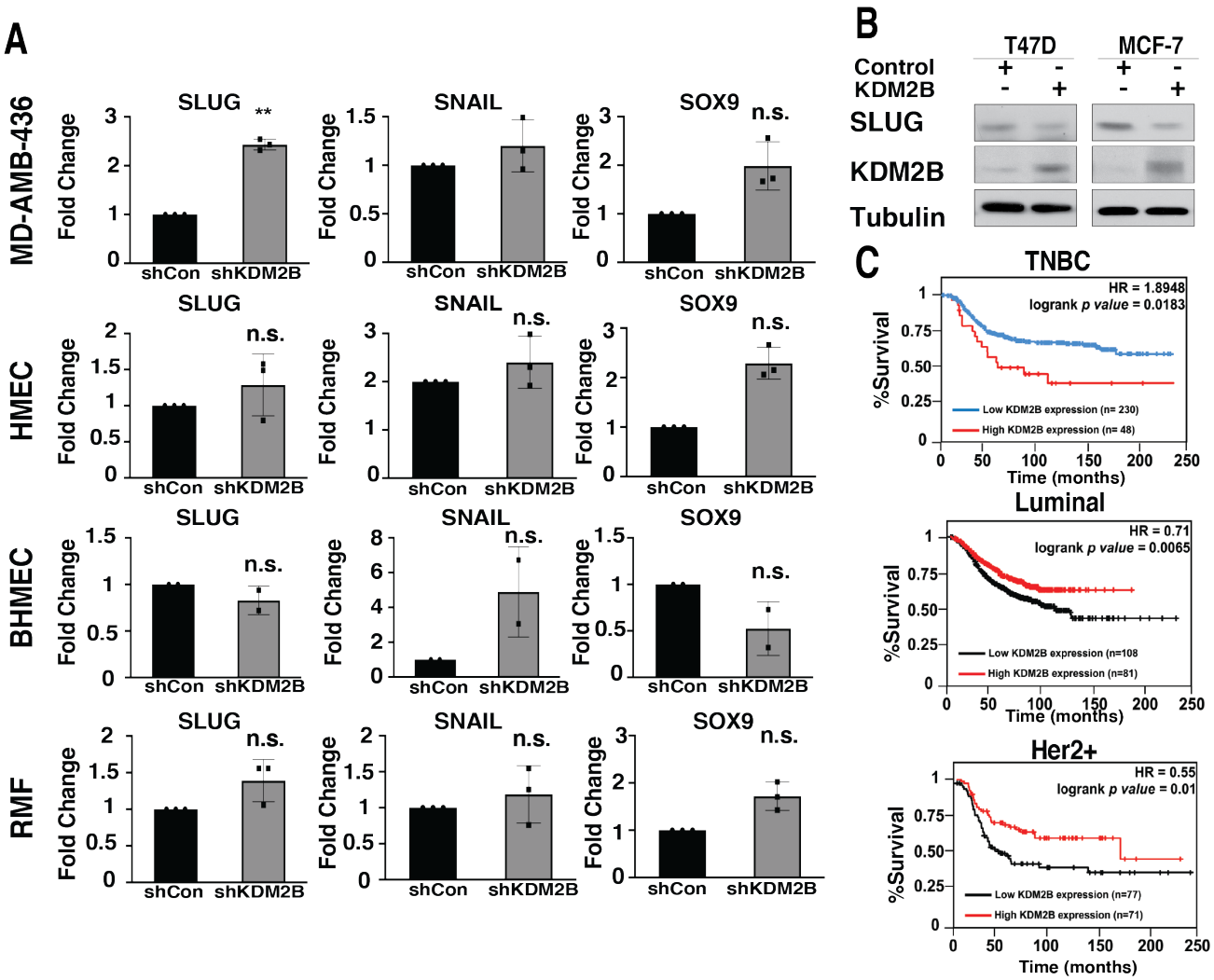

Figure S1: KDM2B regulates SLUG, SNAIL and SOX9 postranscriptionally. Differential role of KDM2B in the regulation of SLUG and in the biology of different types of breast cancer: A. Quantitative RT-PCR failed to detect consistent downregulation of SLUG, SNAIL and SOX9 in shKDM2B-transduced MDA-MB-436, HMEC and BHMEC cells. B. The luminal breast cancer cell lines T47D and MCF-7 were transduced with Control or KDM2B lentiviral constructs. Probing western blots of cell lysates derived from these cell lines with anti-KDM2B, or anti-SLUG antibodies, revealed that KDM2B overexpression promotes the downregulation rather than the upregulation of SLUG. C. Kaplan Meier survival curves of patients with different types of breast cancer, expressing high and low levels of KDM2B, show that whereas KDM2B expression is a predictor of poor prognosis in basal-

like breast cancer, it is a favorable prognostic indicator in luminal and HER2+ tumors. Curves were drawn using the Kaplan Meir Plotter (Nagy et al., 2018) https://kmplot.com/analysis/.

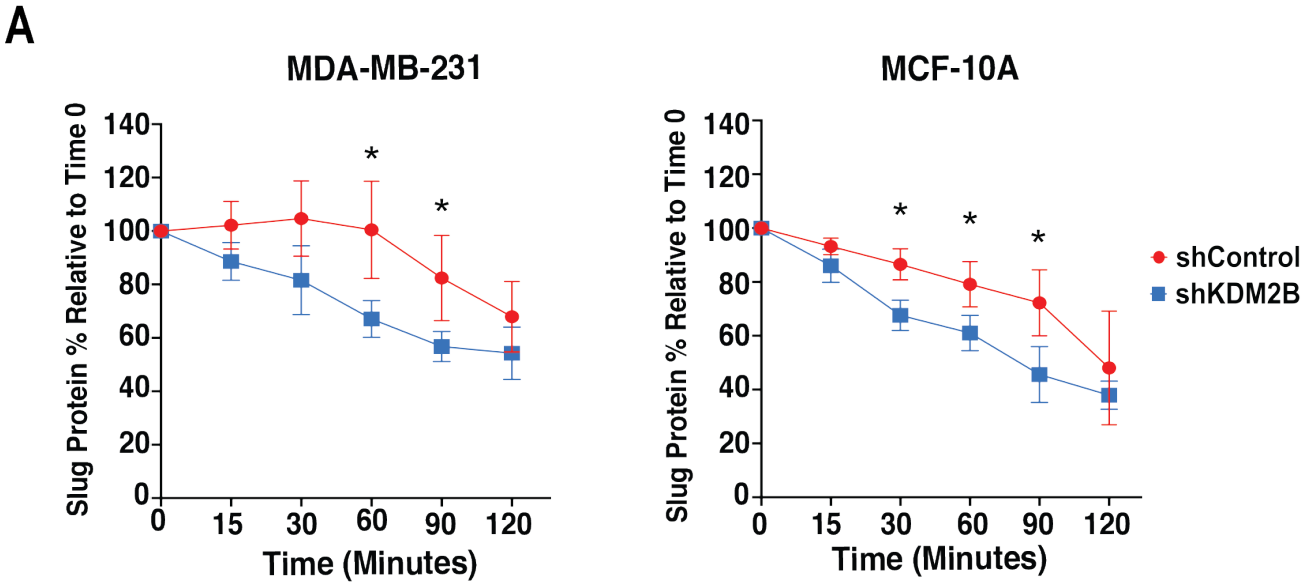

Figure S2: KDM2B knockdown destabilizes SLUG via proteasome-independent mechanisms: Quantification of the western blots in figure 2A confirmed that the degradation of SLUG is more rapid in shKDM2B-transduced, than in shCntrl-transduced MDA-MB-231 (Left panel) and MCF-10A cells (Right panel). Data presented as Mean±SD of values from three independent experiments. Asterisks indicate p-value ≤0.05.

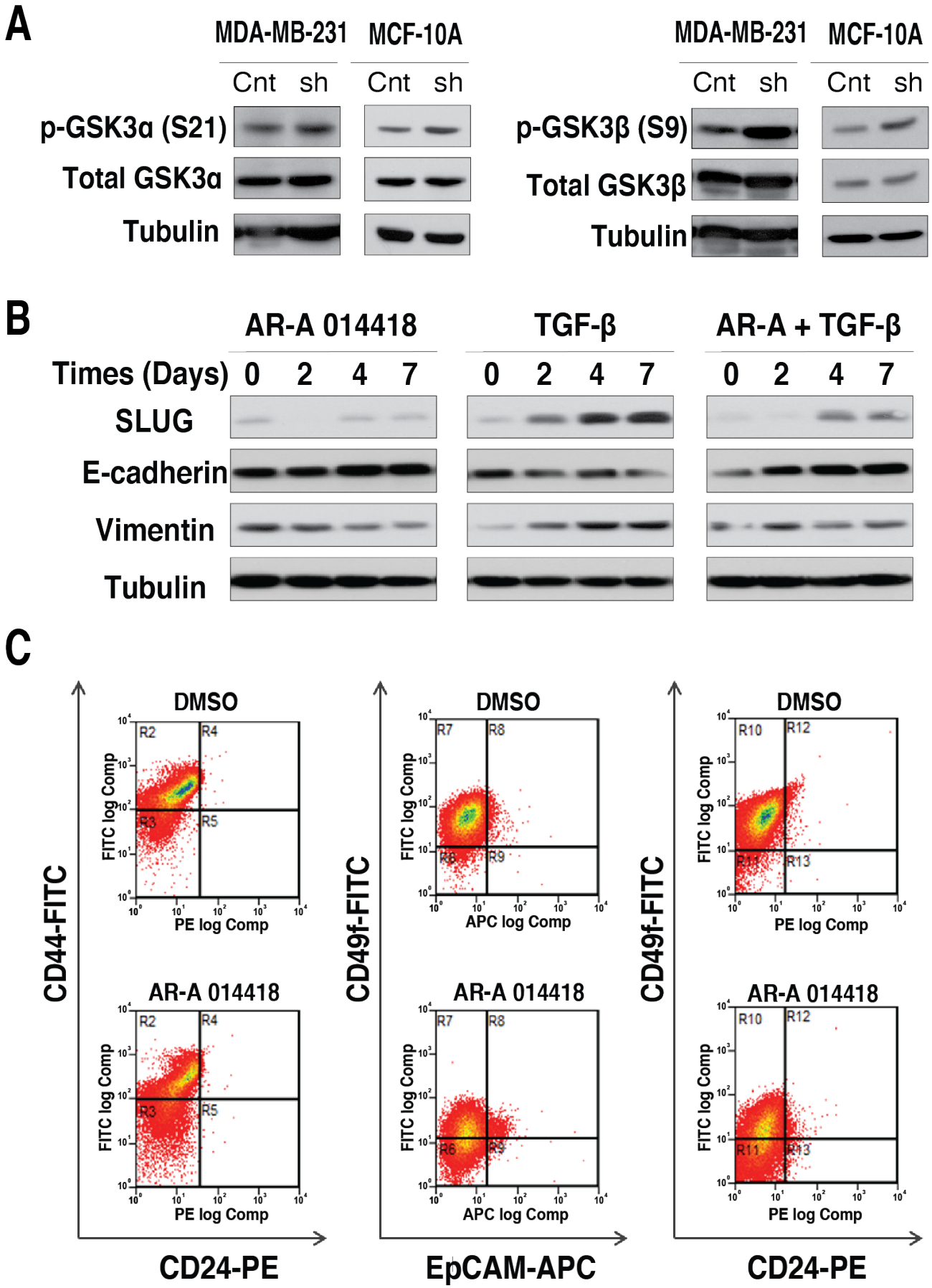
A
MDA-MB-231
MCF-10A
Cnt
sh
p-GSK3α (S21)
Total GSK3α
Tubulin
p-GSK3β (S9)
Total GSK3β
B
AR-A 014418
TGF-β
AR-A + TGF-β
Times (Days)
0
2
4
7
SLUG
E-cadherin
Vimentin
C
DMSO
AR-A 014418
CD44-FITC
CD49f-FITC
FITC log Comp
PE log Comp
APC log Comp
CD24-PE
EpCAM-APC
R2
R3
R4
R5
R6
R7
R8
R9
R10
R11
R12
R13

Figure S3: GSK3β inactivation promotes the differentiation of MCF10A and MDA-MB-231 cells in culture and inhibits TGFβ-induced EMT in MCF10A cells. A. Probing immunoblots of cell lysates derived from MDA-MB-231 and MCF-10A cells transduced with shCntrl, or shKDM2B lentiviral constructs with anti-phospho-GSK3α (Ser21) (Left panel), or anti-phospho-GSK3β (Ser9) (Right panel) antibodies, revealed that shKDM2B promotes the phosphorylation of both, although the phosphorylation of GSK3β is more robust. Antibodies to total GSK3α, GSK3β and tubulin were used as controls. **B.** *(Left panel)* MCF10A cells, which are known to express basal/myoepithelial markers (Qu et al., 2015), were treated with the GSK3 inhibitor AR-A-14418 (2 μM) for seven days and they were harvested at the indicated time points. Probing the cell lysates with the indicated antibodies, revealed a robust, but transient downregulation of SLUG at day 2, a gradual upregulation of E-Cadherin and a gradual downregulation of vimentin, suggesting that GSK3 inhibition induces mesenchymal to epithelial transition (MET). *(Middle panel).* MCF-10A cells were treated with TGFβ (4 ng/ml) and they were harvested at the indicated time points. Probing immunoblots of the lysates with the indicated antibodies, confirmed that TGFβ induces EMT, as determined by the gradual upregulation of SLUG and Vimentin and the gradual downregulation of E-Cadherin. *(Right panel)* Repeating the experiment in the middle panel in the presence of AR-A 14418, revealed that inhibition of GSK3 interferes with the induction of EMT by TGFβ. **C.** MDAMB-231 cells were treated with AR-A-14418 (2 μM) or DMSO. Seven days later the cells were stained with the indicated FITC- and PE or APC-conjugated antibodies (CD44/CD24, CD49f/EpCAM or CD49f/CD24) and they were analyzed by flow-cytometry.

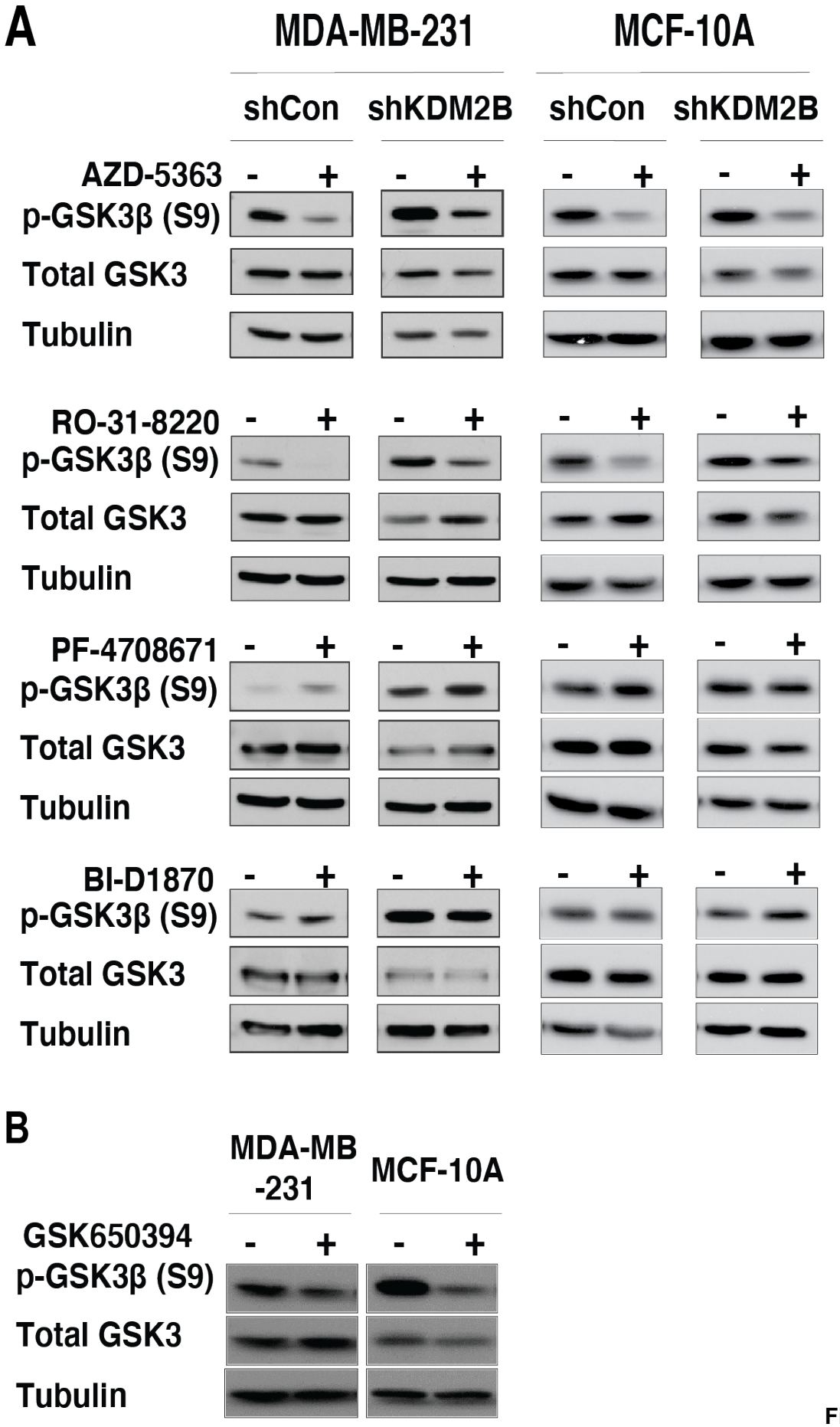
A
MDA-MB-231
MCF-10A
shCon
shKDM2B
shCon
shKDM2B
AZD-5363
- + - + - + - +
p-GSK3β (S9)
Total GSK3
Tubulin
RO-31-8220
- + - + - + - +
p-GSK3β (S9)
Total GSK3
Tubulin
PF-4708671
- + - + - + - +
p-GSK3β (S9)
Total GSK3
Tubulin
BI-D1870
- + - + - + - +
p-GSK3β (S9)
Total GSK3
Tubulin
B
MDA-MB -231
MCF-10A
GSK650394
- + - +
p-GSK3β (S9)
Total GSK3
Tubulin

Figure S4:

Steady state phosphorylation of GSK3β in MDA-MB-231 and MCF-10A cells is mediated by AKT, PKC and SGK: A. MDA-MB-231 and MCF-10A cells transduced with shCntrl or shKDM2B constructs, were treated with the indicated kinase inhibitors (pan AKT, AZD-5363 (0.5 μM); Classical PKC, RO-31-8220 (0.1 μM); p70S6K, PF-4708671 (10 μM) and p90RSK, BI-D1870 (10 μM)). Probing immunoblots of cell lysates harvested at two hours from the start of the treatment, revealed that AKT and PKC phosphorylate GSK3 in both the shCntrl and shKDM2B cells. **B.** Probing with the same antibodies cell lysates of the same cells, following a 24 hour treatment with the SGK inhibitor GSK650394 (10 μM), revealed that SGK also promotes the steady state phosphorylation of GSK3.

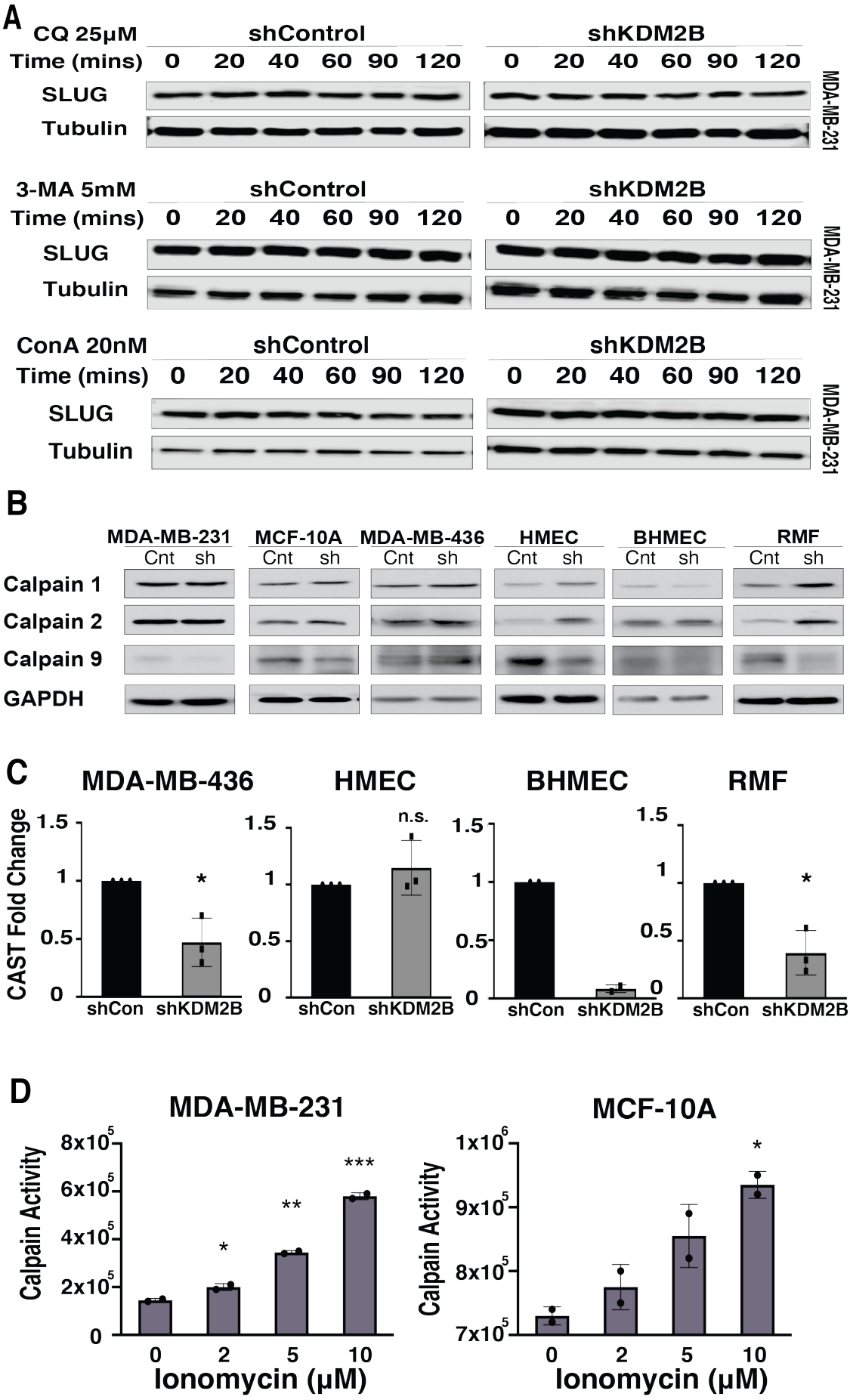
A
CQ 25μM
shControl
shKDM2B
Time (mins) 0 20 40 60 90 120 0 20 40 60 90 120
SLUG
Tubulin
MDA-MB-231
3-MA 5mM
shControl
shKDM2B
Time (mins) 0 20 40 60 90 120 0 20 40 60 90 120
SLUG
Tubulin
MDA-MB-231
ConA 20nM
shControl
shKDM2B
Time (mins) 0 20 40 60 90 120 0 20 40 60 90 120
SLUG
Tubulin
MDA-MB-231
B
MDA-MB-231
MCF-10A
MDA-MB-436
HMEC
BHMEC
RMF
Cnt sh
Calpain 1
Calpain 2
Calpain 9
GAPDH
C
MDA-MB-436
HMEC
BHMEC
RMF
CAST Fold Change
1.5
1
0.5
0
*
n.s.
shCon shKDM2B
D
MDA-MB-231
MCF-10A
Calpain Activity
8x10^5
6x10^5
4x10^5
2x10^5
0
1x10^6
9x10^5
8x10^5
7x10^5
*
**
***
0 2 5 10
Ionomycin (μM)

Figure S5: The shKDM2B-induced degradation of SLUG is calpain-mediated. A. MDA-MB-231 cells transduced with shCntrl or shKDM2B constructs were treated with cloroquine (CQ), 3-methyladenine (3-MA) or concanamycin A at the indicated concentrations. Probing immunoblots of cell lysates harvested at the indicated time points from the start of the treatment, with anti-SLUG or anti-GAPDH (loading control) antibodies, revealed that none of the autophagy inhibitors rescued the shKDM2B-induced destabilization of SLUG. **B.** All six cell lines in our panel were transduced with shCntrl or shKDM2B. Probing immunoblots of lysates derived from these cells with anti-calpain 1, 2 or 9 antibodies, revealed that whereas Calpain 1 and 2 were upregulated in some cell lines, calpain 9 was downregulated in all. **C.** Measurement of the calpastatin mRNA levels by quantitative RT-PCR in shCntrl and shKDM2B-transduced MDA-MB-436, HMEC, BHMEC and RMF cells, confirmed that calpastatin is downregulated by KDM2B at the RNA level in all the cell lines, except of HMEC. Data are presented as mean ± SD and asterisks indicate statistical significance (p-value ≤ 0.05). **D.** MDAMB-231 and MCF-10A cells were treated with increasing concentrations of ionomycin, as indicated. Calpain 1 and 2 activity was measured in cell lysates harvested at 1 hour from the start of the ionomycin treatment, using a luminescent assay. Data are presented as mean ± SD and asterisks indicate statistical significance (* p-value ≤ 0.05, ** p-value ≤ 0.01, *** p-value ≤ 0.001).

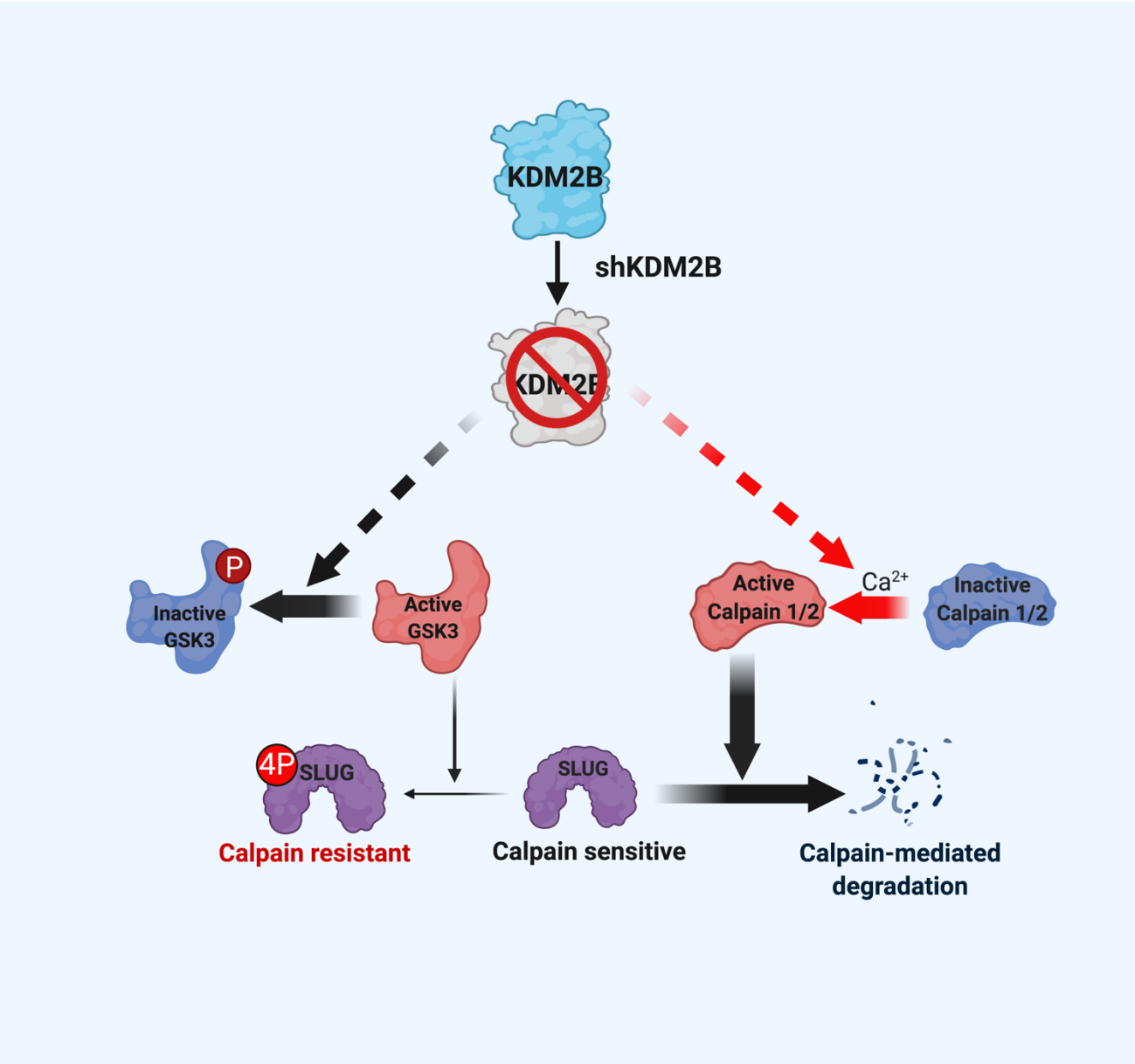

Figure S6. Proposed model of Calpain-mediated SLUG cleavage induced by the knockdown of KDM2B. The knockdown of KDM2B results in the inactivation of GSK3 and the activation of calpain. Both of these pathways converge on SLUG and promote its degradation. By inactivating GSK3, the knockdown of KDM2B blocks SLUG phosphorylation and renders SLUG sensitive to calpain-mediated cleavage. Therefore, the inactivation of GSK3 increases the calpain sensitivity of SLUG and acts synergistically with the activated calpain.

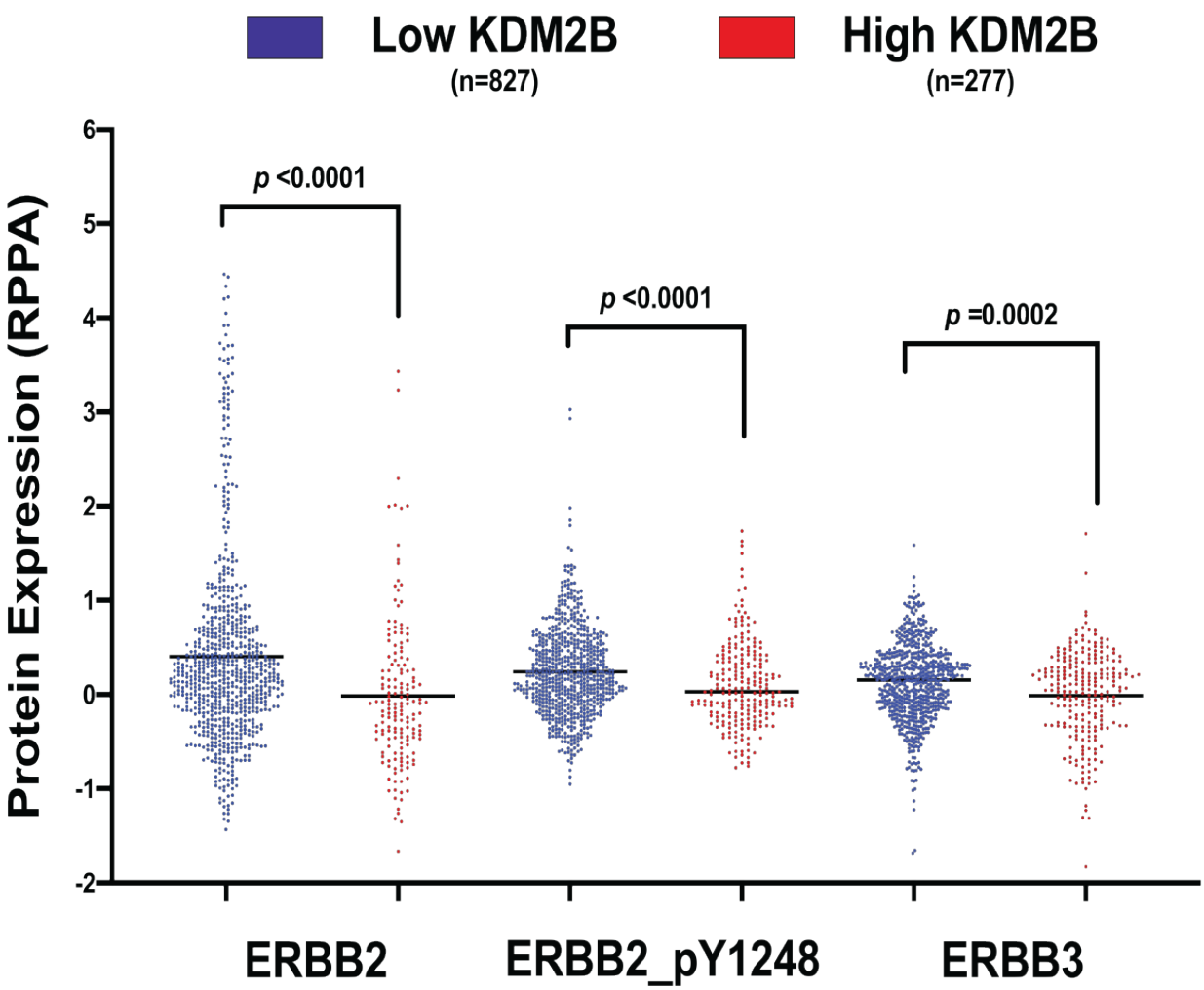

Figure S7. Abundance of ERBB2, ERBB2_pY1248 and ERBB3, in human mammary adenocarcinomas expressing high, or low levels of KDM2B. Distribution of the abundance of ERBB2, ERBB2_pY1248 and ERBB3 in human mammary adenocarcinomas expressing high (Brown) or low (Blue) levels of KDM2B. Horizontal lines indicate the mean values. Tumors with low KDM2B tend to express higher levels of ERBB2, ERBB2_pY1248 and ERBB3, than tumors with high KDM2B. Statistical analysis was performed using the unpaired one tail student's t test.